ICML 2025

Thickness-aware E(3)-Equivariant 3D Mesh Neural Network

Sungwon Kim, Namkyeong Lee, Yunyoung Doh, Seungmin Shin
Guimok Cho, Seung-Won Jeon, Sangkook Kim, Chanyoung Park

Presenter: Sungwon Kim

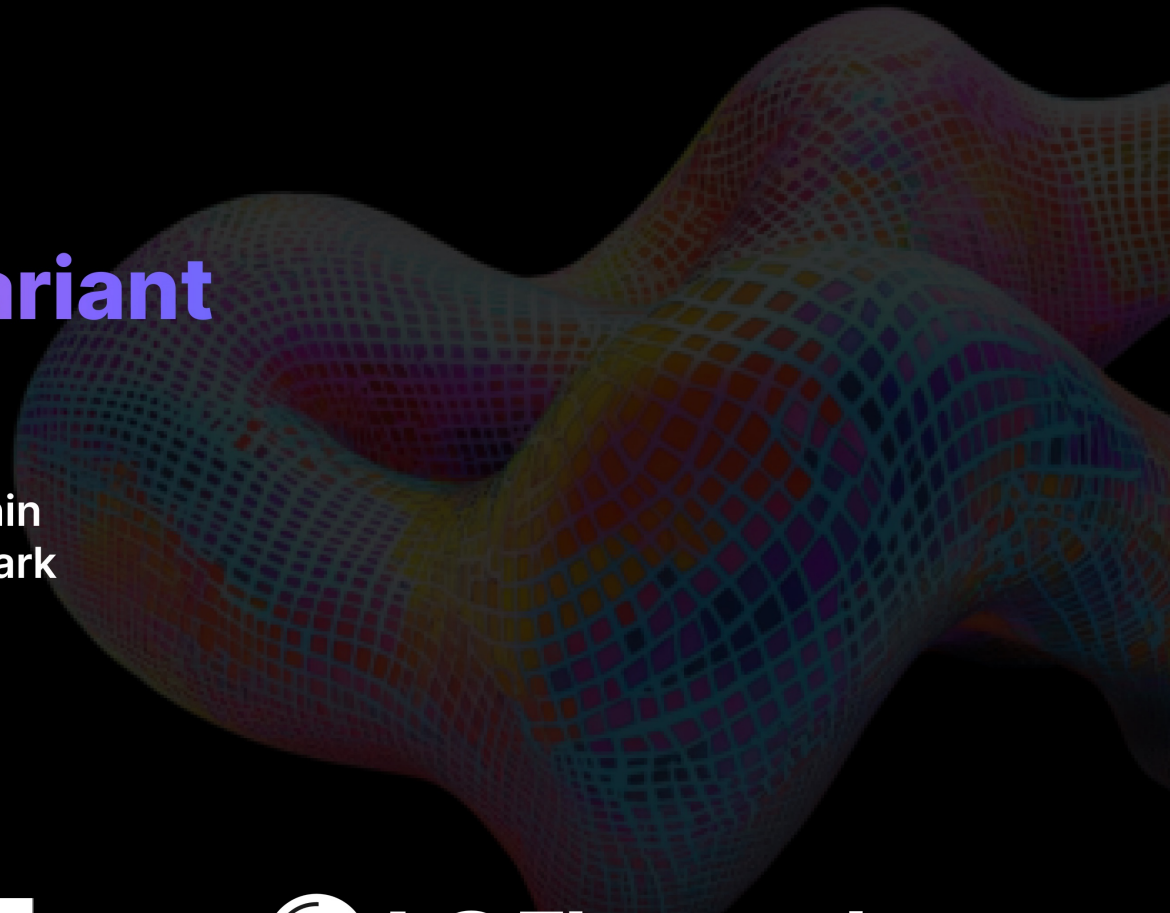

ICML International Conference On Machine Learning

KAIST

LG Electronics

WHY 3D SIMULATION MATTERS

- **The role of static analysis in manufacturing**

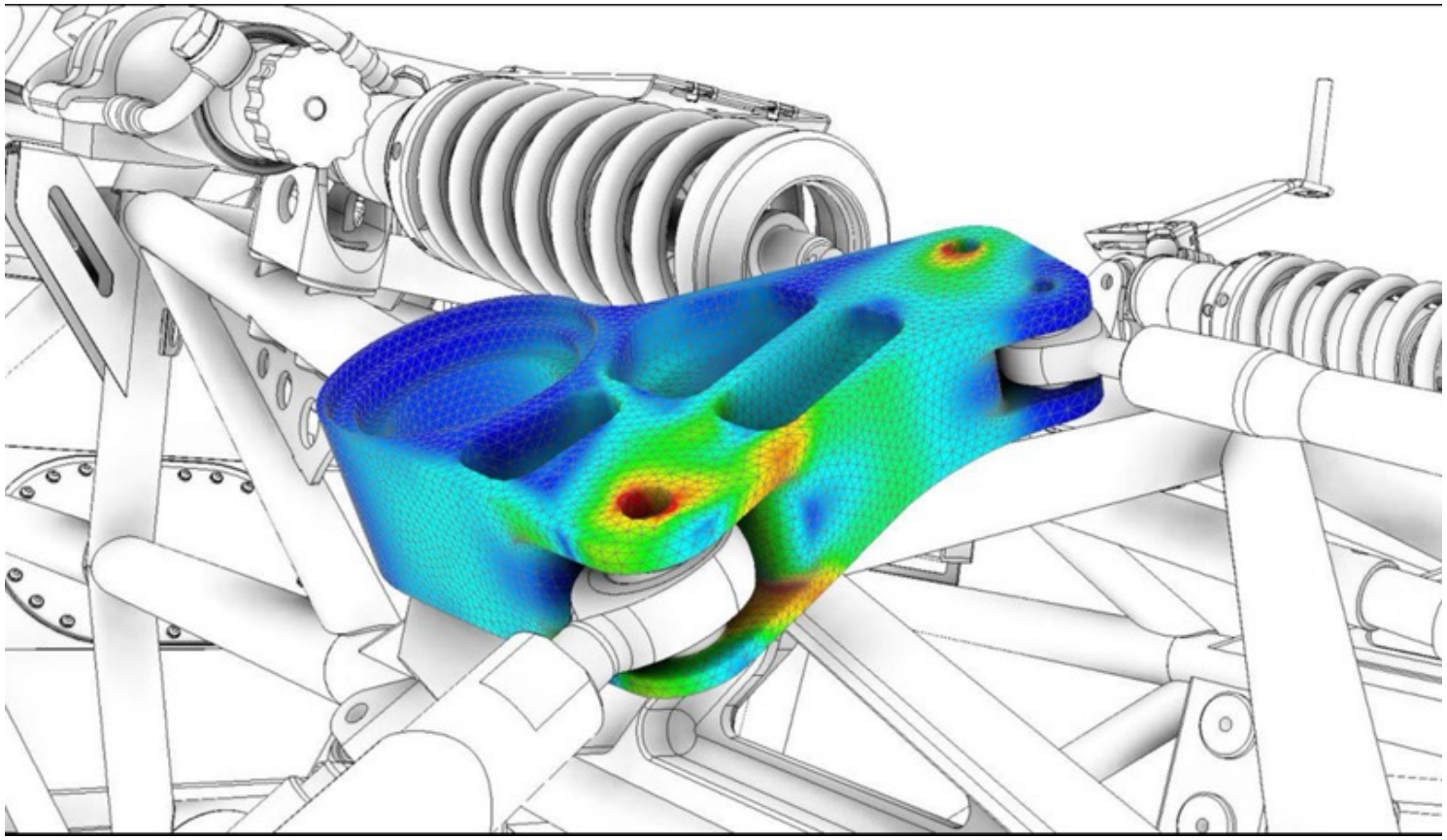

Analysis & Simulation: Identify **potential product risks** under real-world conditions **before moving into production.**

https://onecadvn.com/en/solutions/3d-design

WHY 3D SIMULATION MATTERS

- **The role of static analysis in manufacturing**

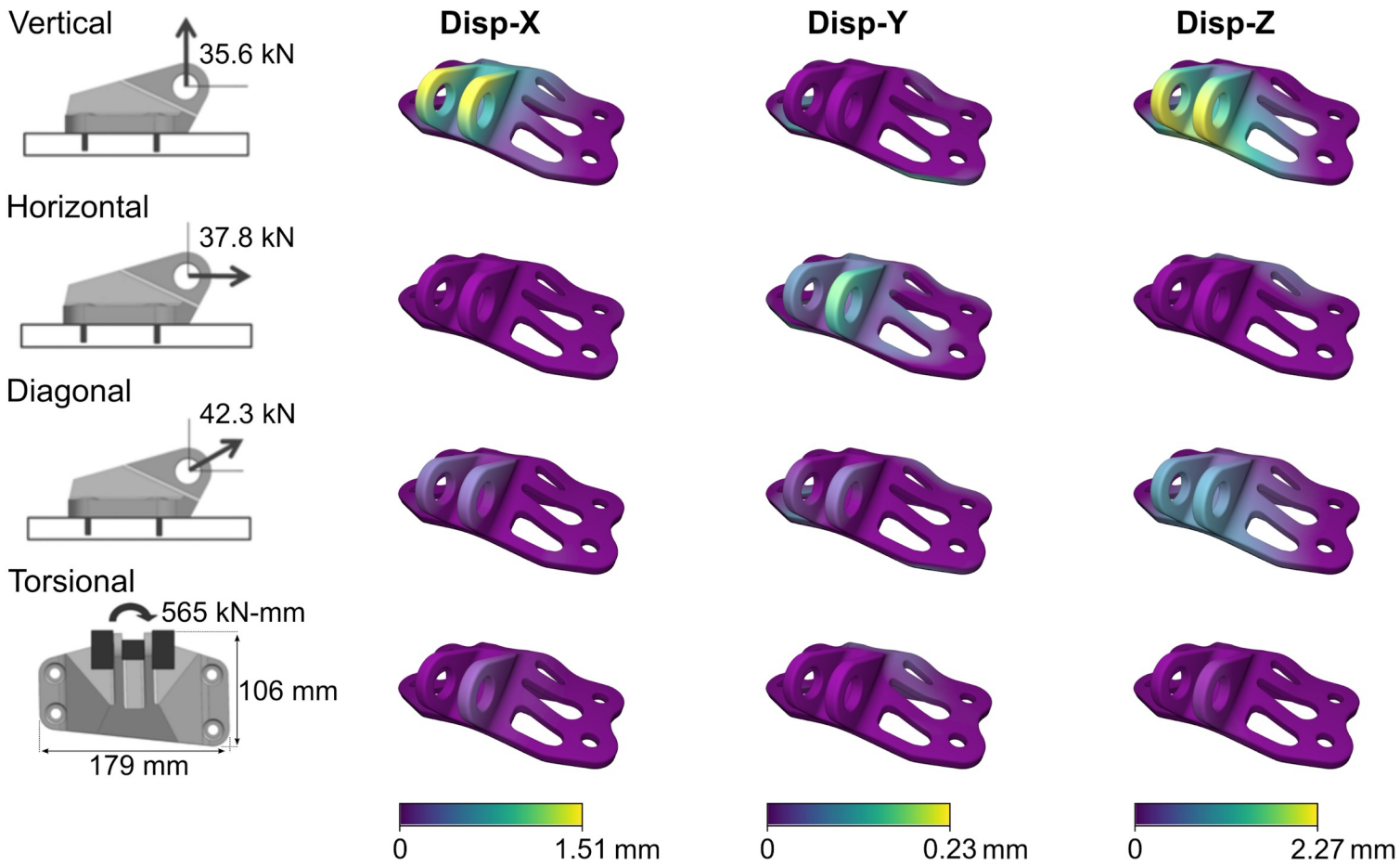

Whalen, Eamon, Azariah Beyene, and Caitlin Mueller. "SimJEB: simulated jet engine bracket dataset." *Computer Graphics Forum*. Vol. 40. No. 5. 2021.

WHY 3D SIMULATION MATTERS

- **The role of static analysis in manufacturing**

	X deflection	Y deflection	Z deflection
Prediction	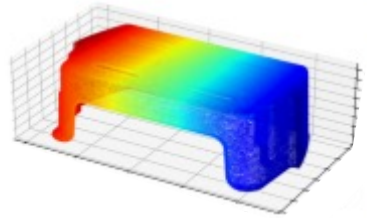	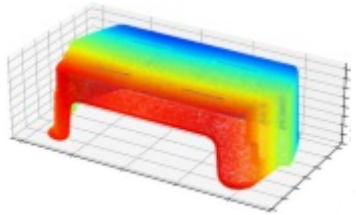	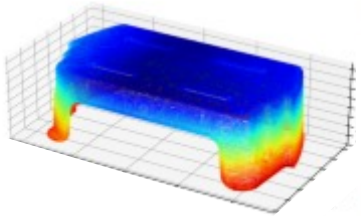
Ground Truth	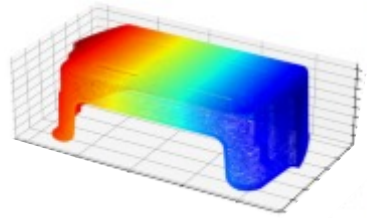	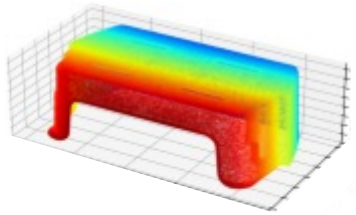	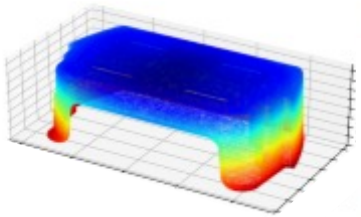
Error	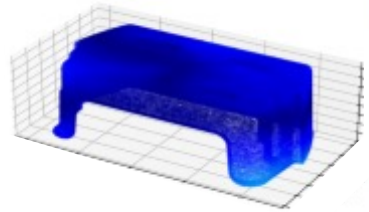	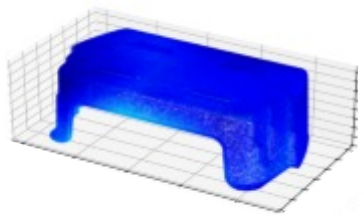	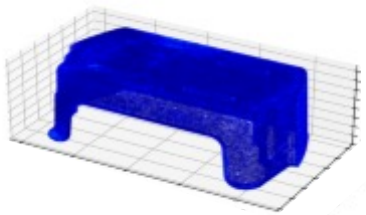

Conditions

- Temperature
- Pressure
- Injected position
- Viscosity
- Conductivity
- Cooling time
- Injection time
- …

WHY 3D SIMULATION MATTERS

- **The role of static analysis in manufacturing**

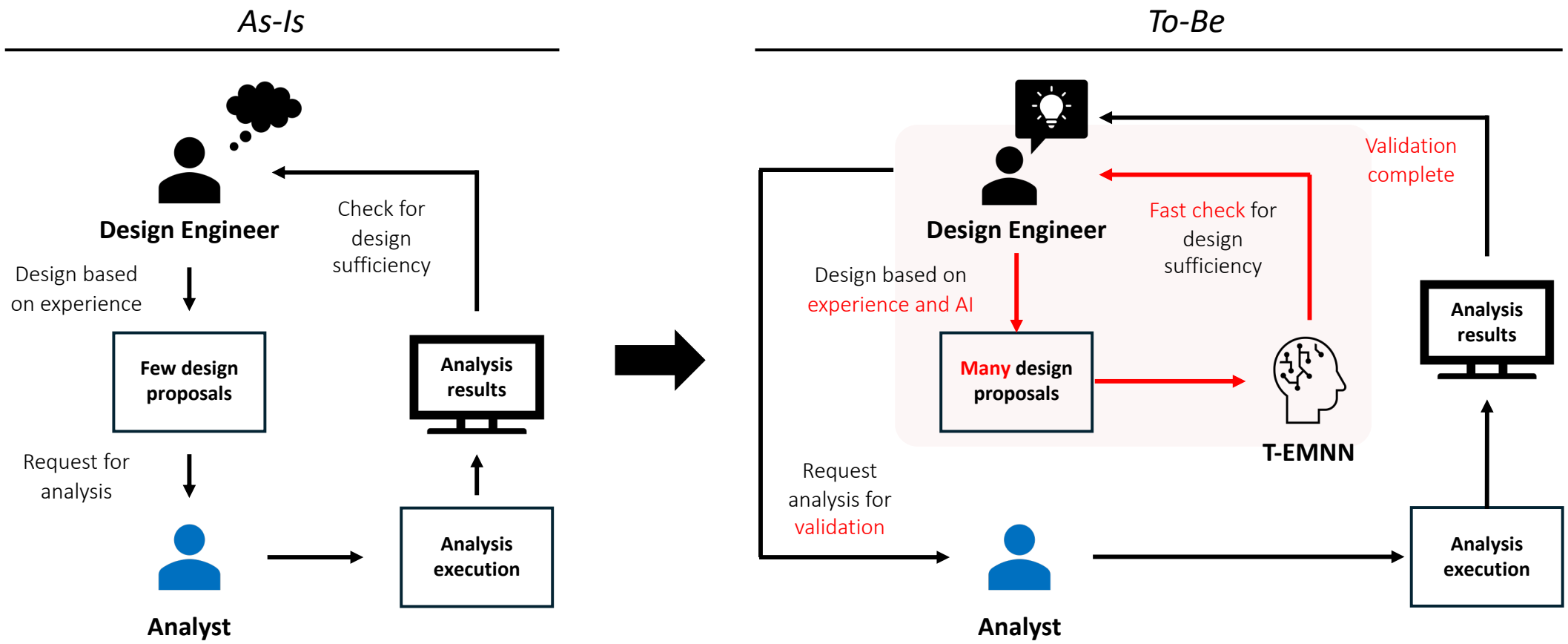

3D simulation is the key to building **better products, faster and cheaper**.

CHALLENGE: CONVENTIONAL SOLVERS

- **Finite Element Method (FEM): High Computational Cost**

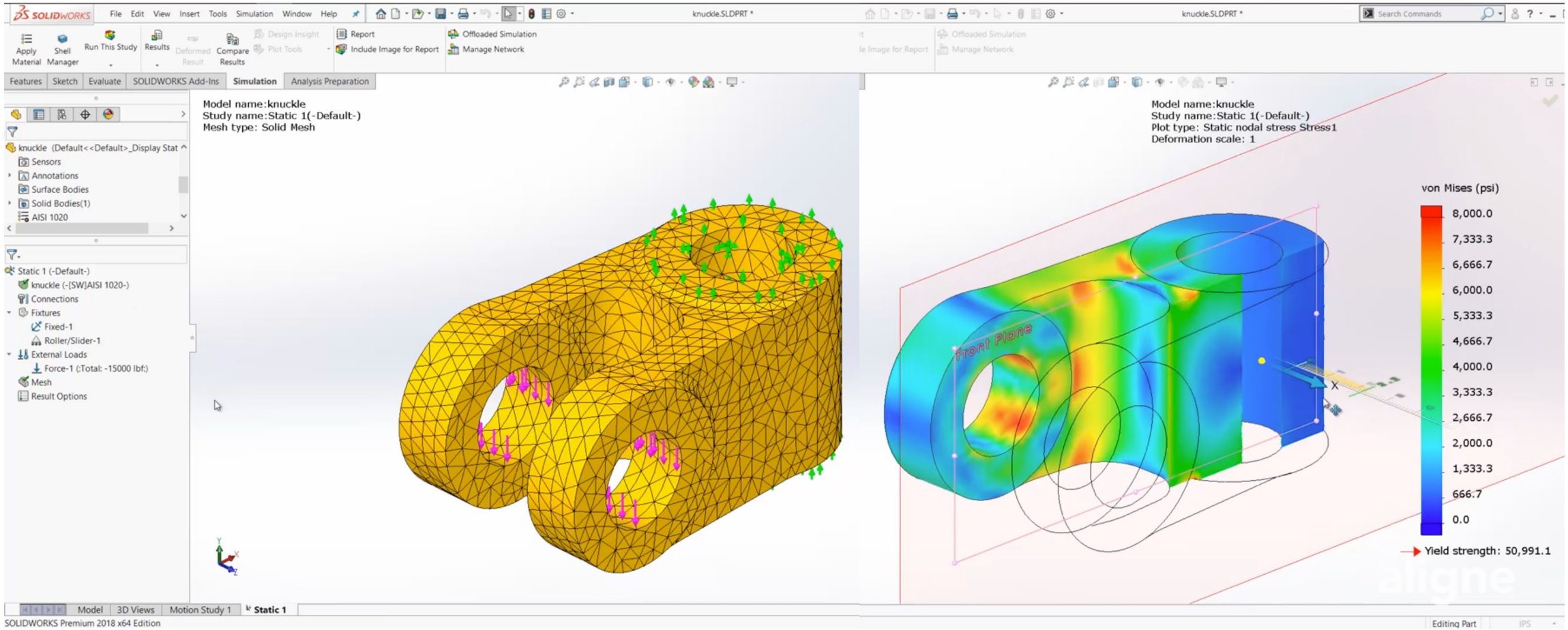

Performing a single FEM analysis involves **high computational costs and extended runtimes.**

CHALLENGE: CONVENTIONAL SOLVERS

- **Finite Element Method (FEM): High Computational Cost**

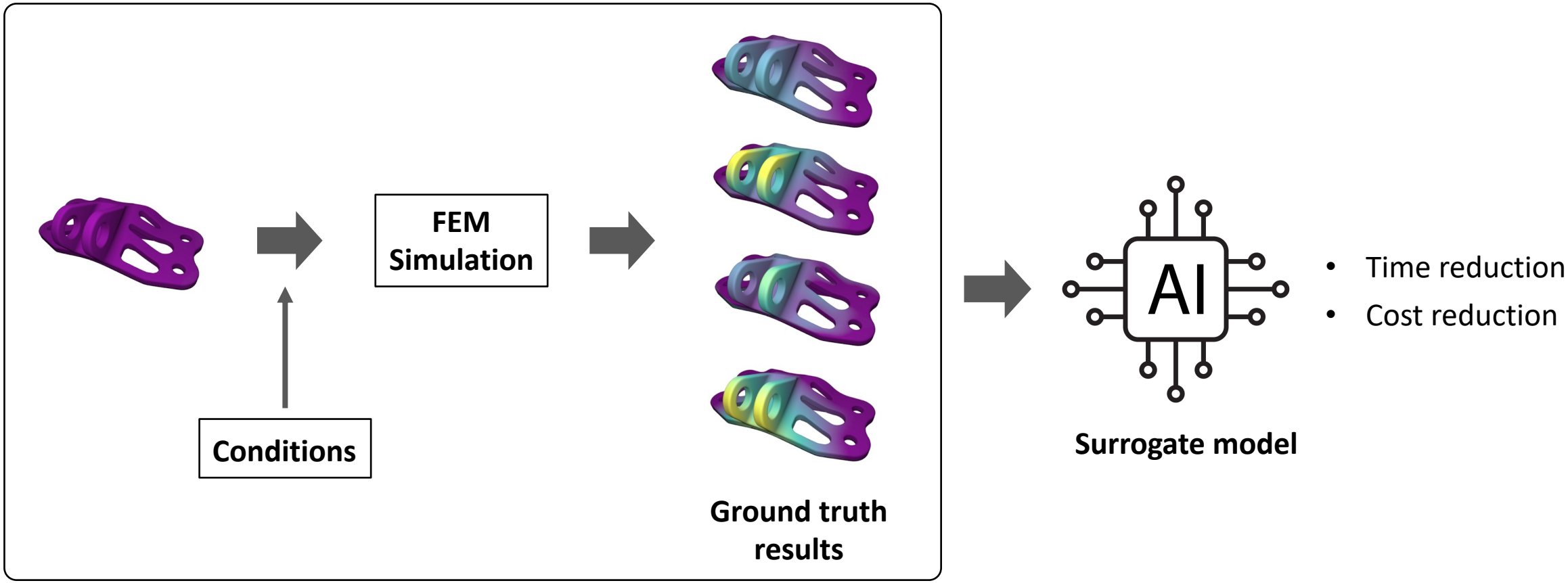

Learning-based AI models can serve as powerful surrogates,
significantly reducing the high computational cost of FEM simulations.

TASK

- **Node-level deflection (3d) prediction**

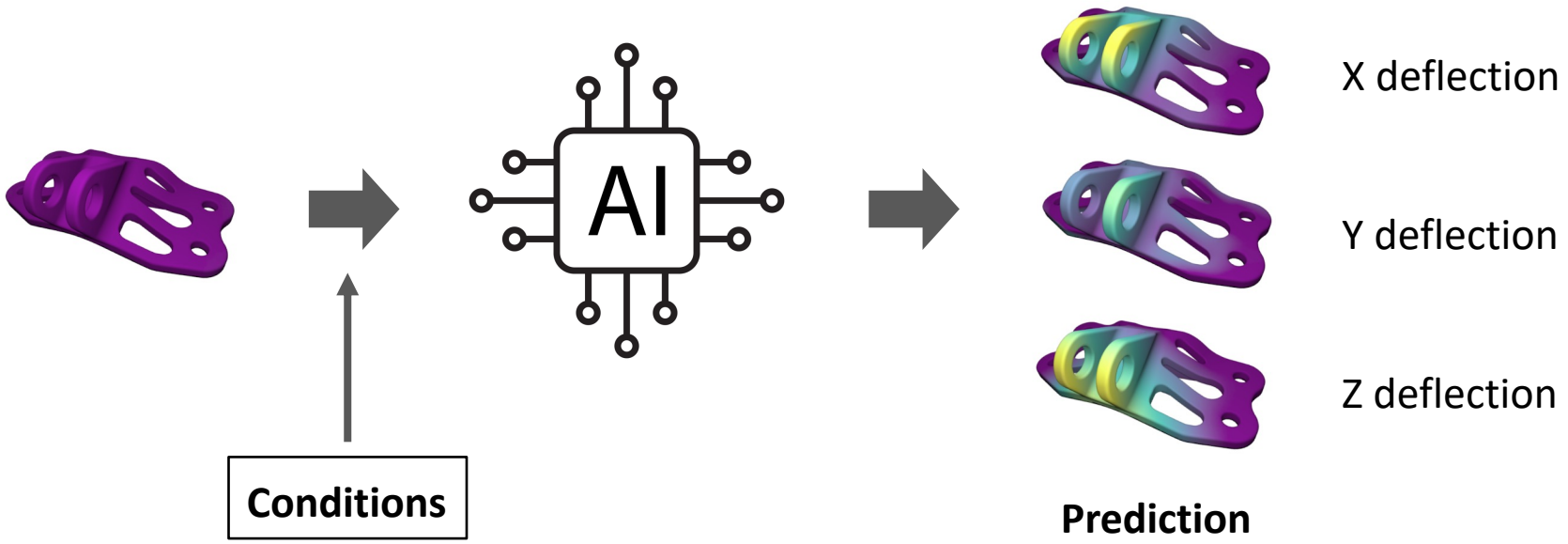

3D REPRESENTATION

- **3D Mesh: Vertices, Edges, and Faces**

Point cloud

Voxel

Polygon mesh

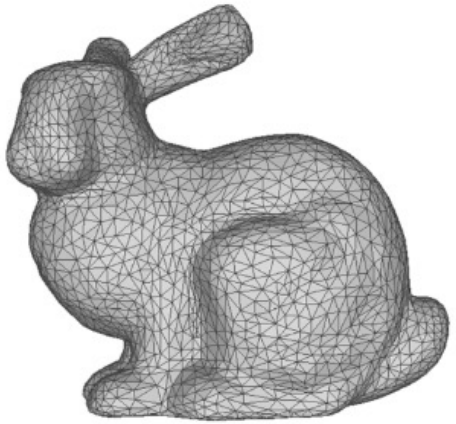

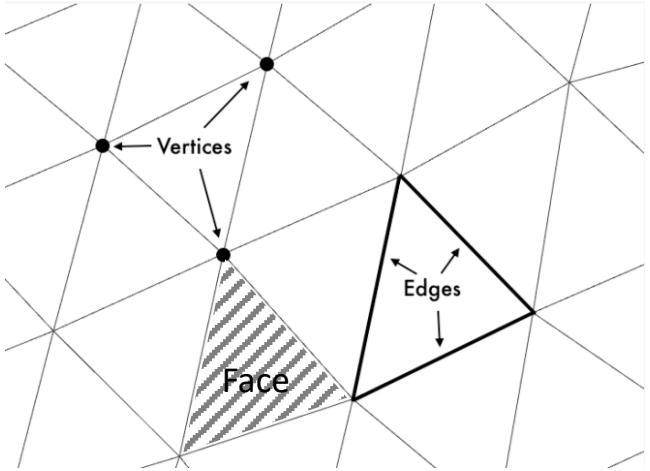

3D Mesh is one the best way to **describe surfaces and volumes of object!**

3D REPRESENTATION

- **3D Mesh: Volume mesh vs. Surface mesh**

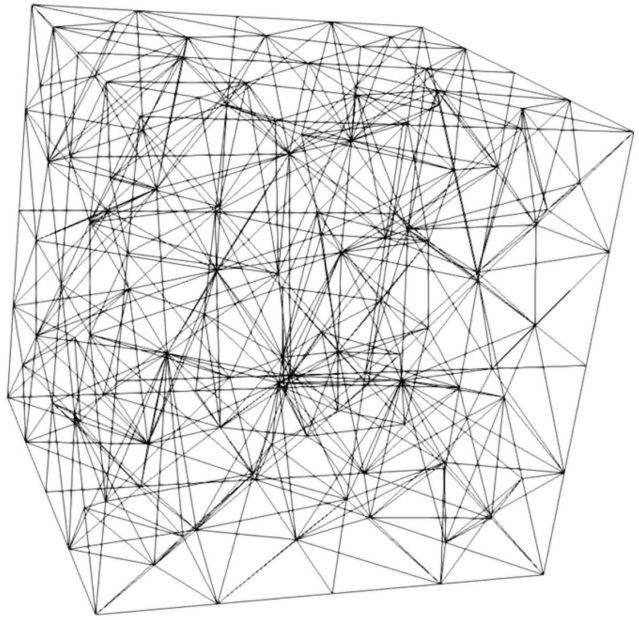

Volume mesh

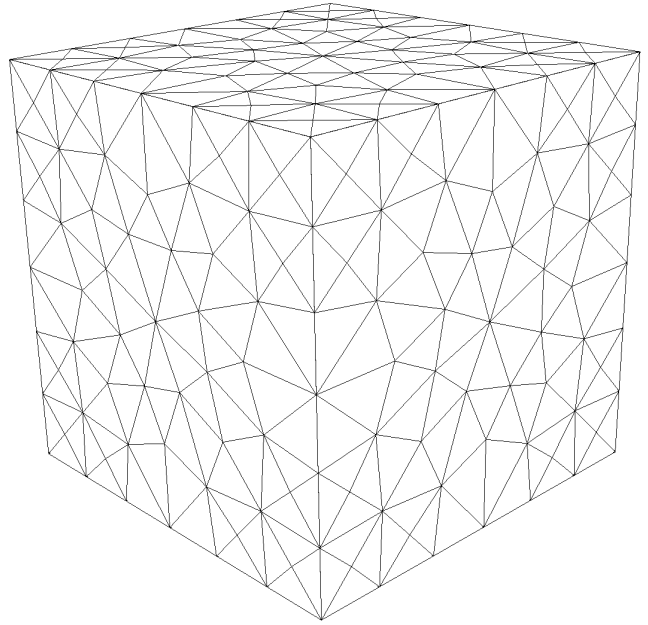

Surface mesh

3D REPRESENTATION

- **3D Mesh: Volume mesh vs. Surface mesh**

Volume mesh

Surface mesh

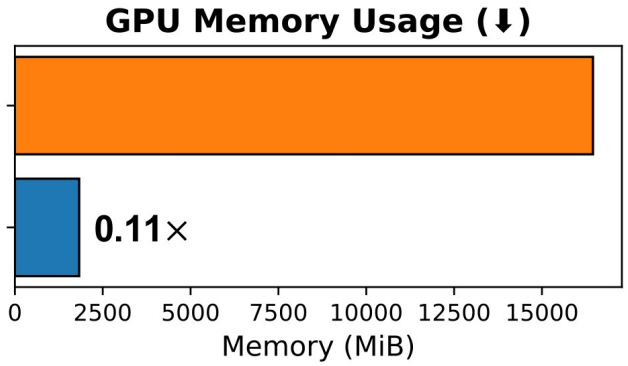

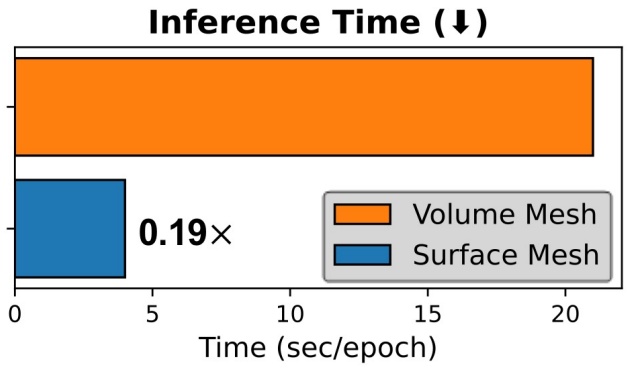

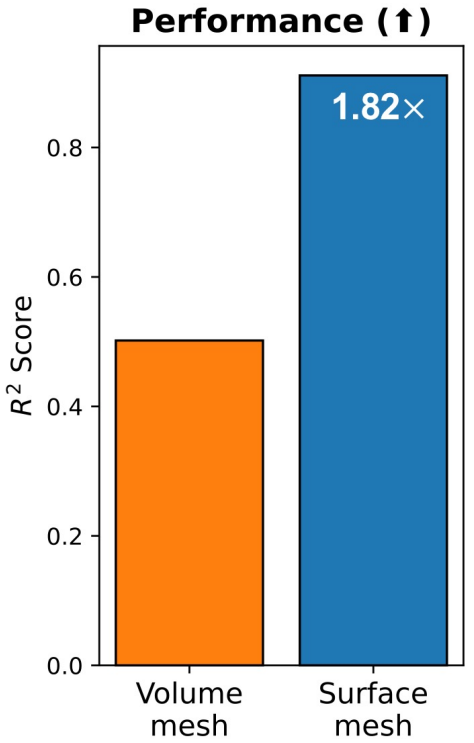

Surface meshes are **significantly faster, more cost-effective,**
and better suited for modeling the **geometric properties** of a shape.

PROBLEM WITH SURFACE MESH

- Ignoring Critical Thickness Information

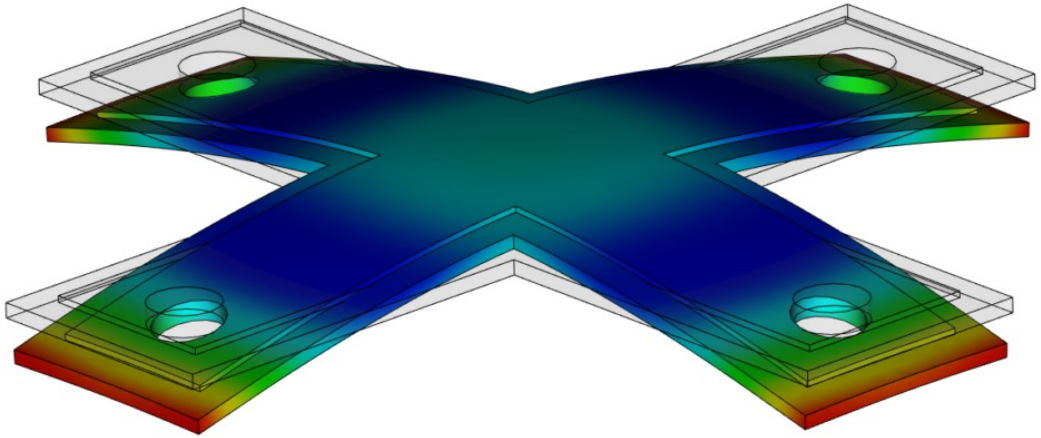

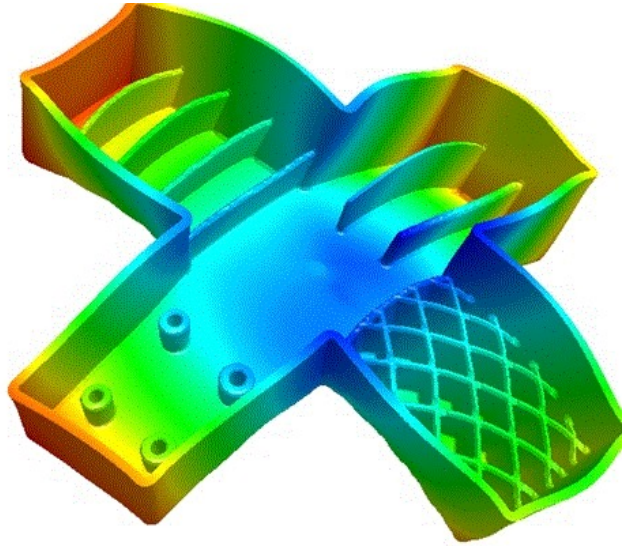

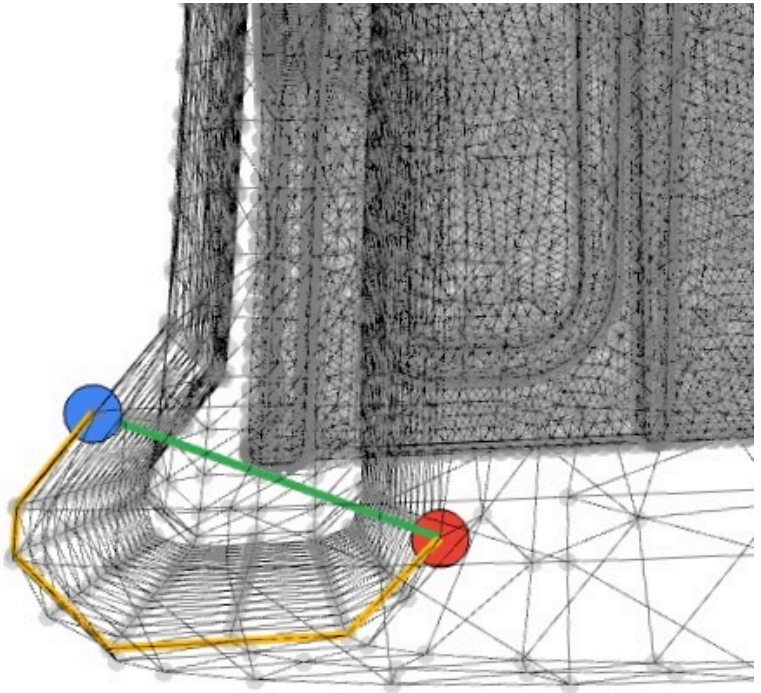

PROBLEM WITH SURFACE MESH

- **Ignoring Critical Thickness Information**

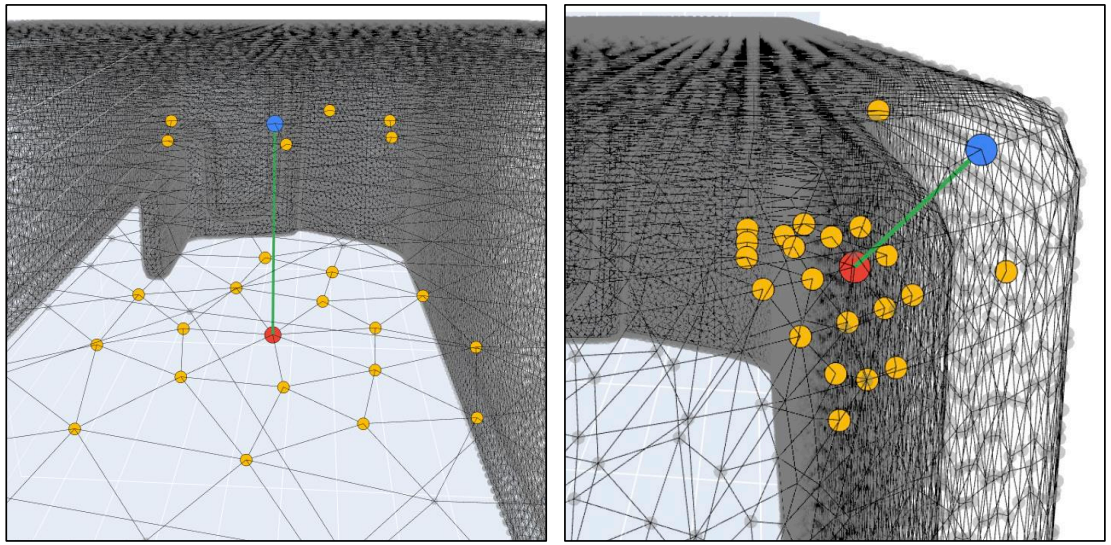

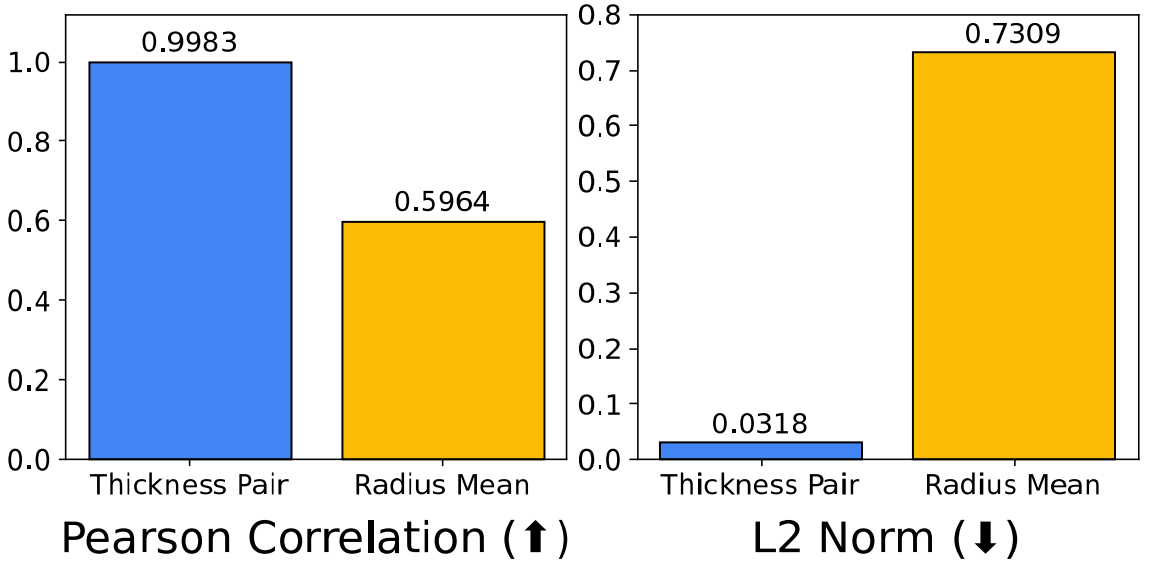

Surface meshes face **challenges in modeling the interactions between thickness pair** due to the lack of connections between opposing surfaces within the mesh

OUR MOTIVATION

- **Bringing the gap between surface mesh efficiency and physical accuracy**

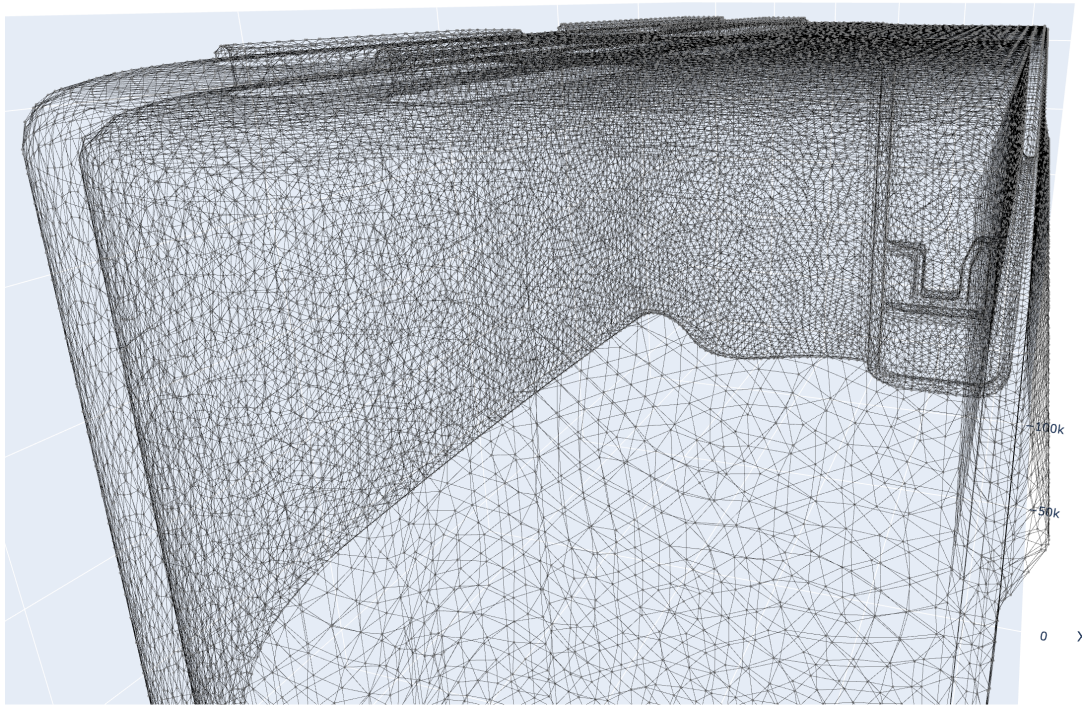

Surface mesh

+

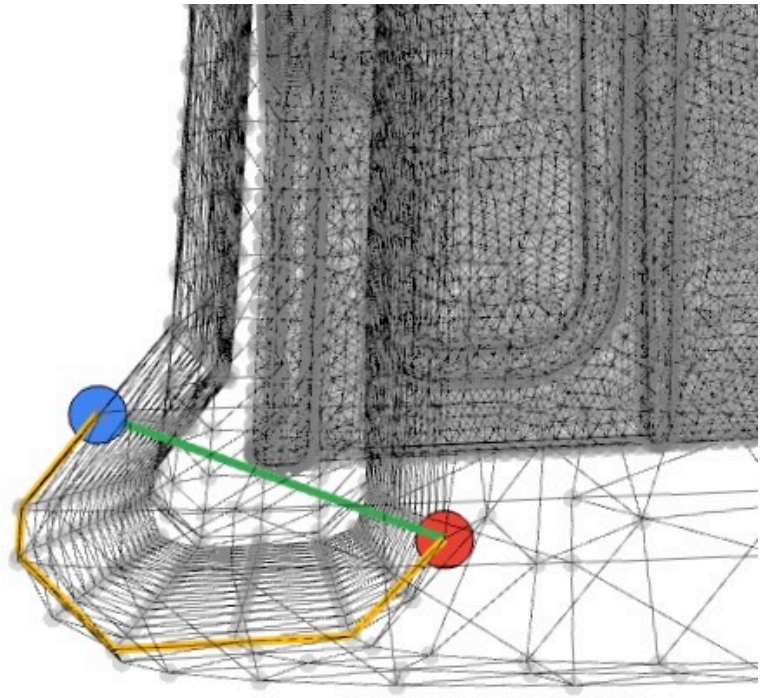

Thickness interaction

We achieve accurate and efficient 3D analysis by modeling
thickness interactions directly on the surface mesh.

PROPOSED METHOD

- **Core Idea 1: Thickness-Awareness**

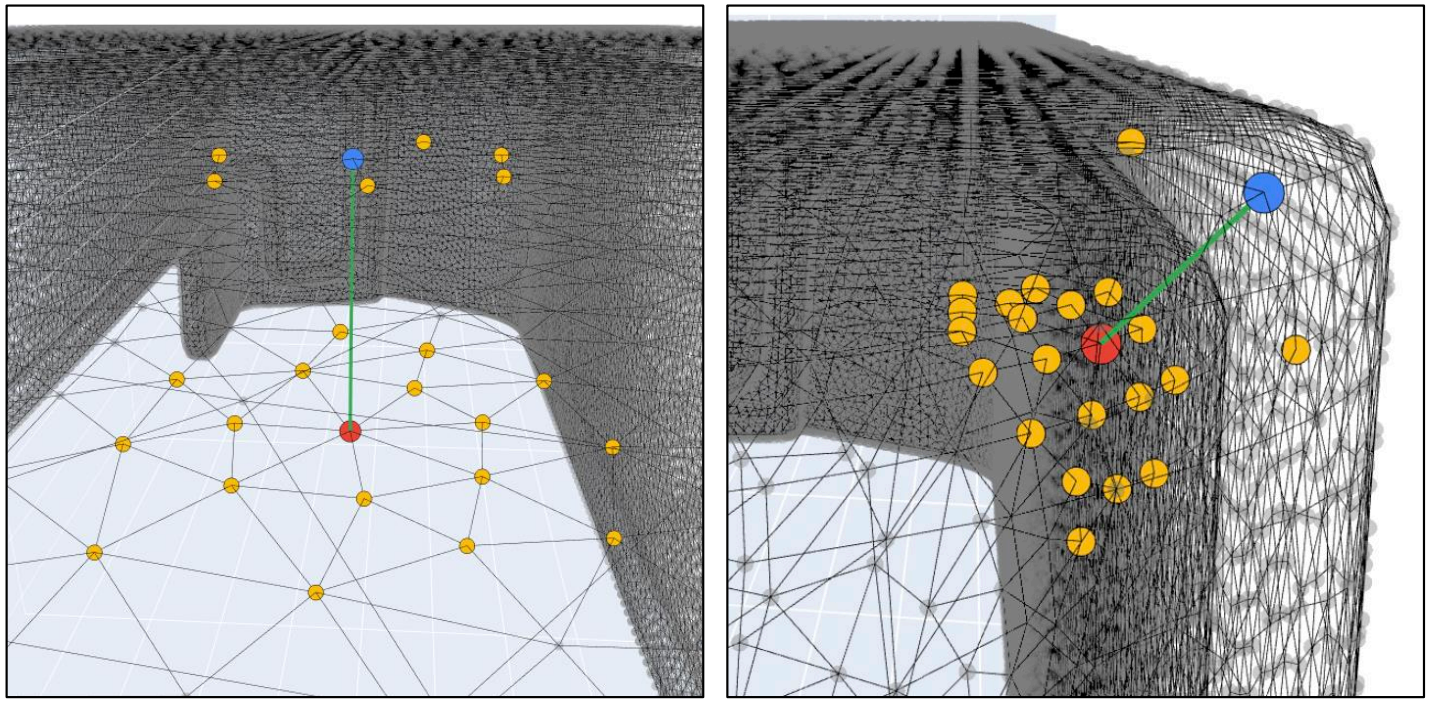

: Thickness pair nodes

: Thickness edges

We introduce a **'thickness edge'** to connect a node with its corresponding 'thickness paired node' on the opposing surface.

PROPOSED METHOD

- **Core Idea 1: Thickness-Awareness**

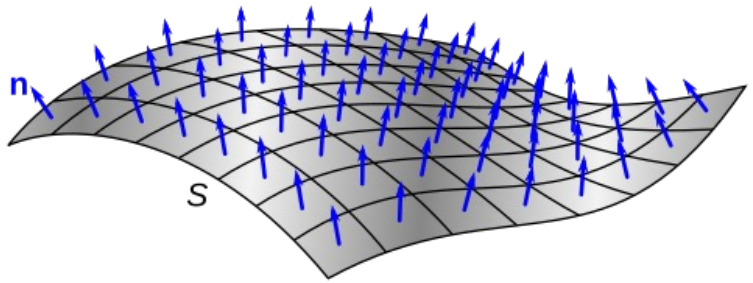

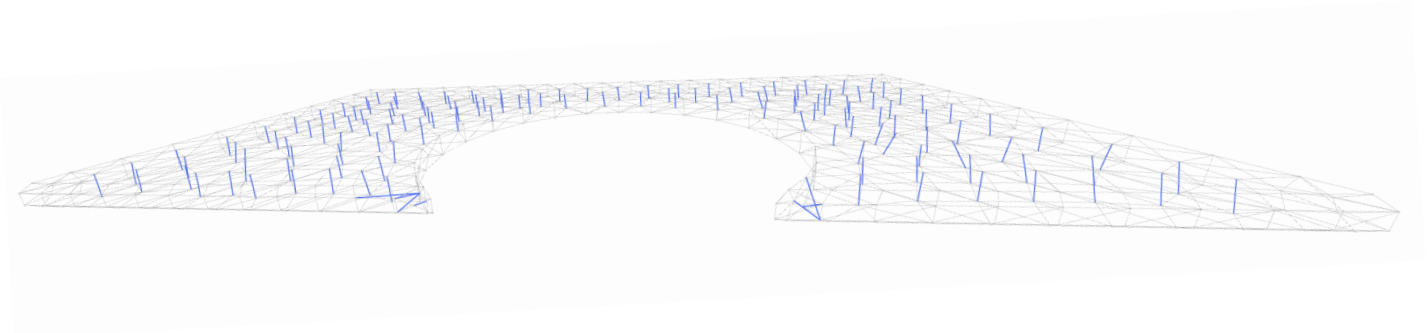

- Definition of a '**thickness paired node**'

$$\mathcal{T}(v_i) = \underset{v_j \in V, v_j \neq v_i}{\arg\min} \left\| \mathbf{x}_j - \left(\mathbf{x}_i - d \cdot \mathbf{n}_i^{\text{node}} \right) \right\|,$$

$$\mathcal{T}(v_i) \in V, \text{ where } \mathcal{T}(v_i) \neq v_i$$

$\mathbf{x}$: coordinate, $\mathbf{n}^{\text{node}}$: normal vector

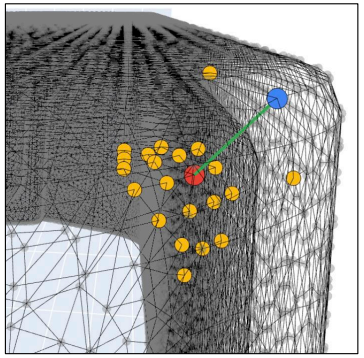

- Definition of a '**thickness**'

$$t(v_i) = \left\| \mathbf{x}_i - \mathbf{x}_{\mathcal{T}(v_i)} \right\|$$

PROPOSED METHOD

- **Core Idea 1: Thickness-Awareness**

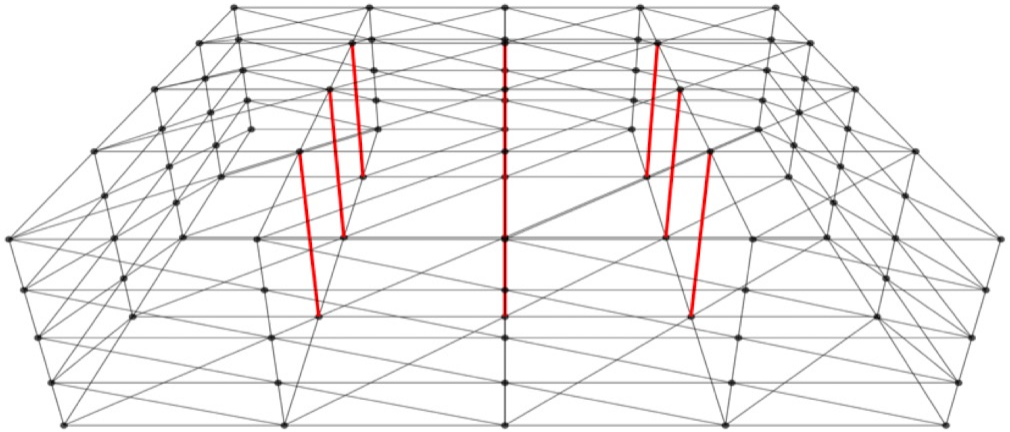

(a) Thickness

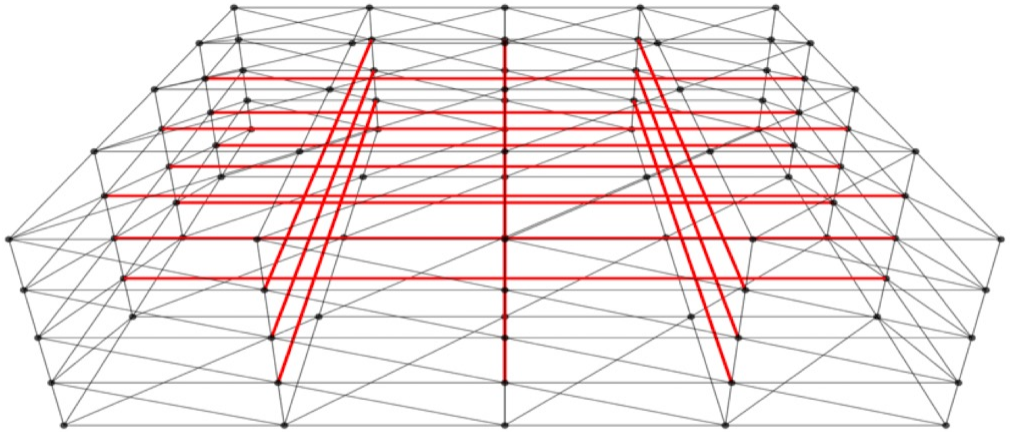

(b) Width

Opposing nodes do not always define true 'thickness'.
They can also represent 'width', which has a weaker dynamic relationship.

PROPOSED METHOD

- **Core Idea 1: Thickness-Awareness**

$$I_i = \frac{1}{1 + e^{\alpha(t(v_i) - \tau)}}$$

τ : learnable threshold for the thickness edge

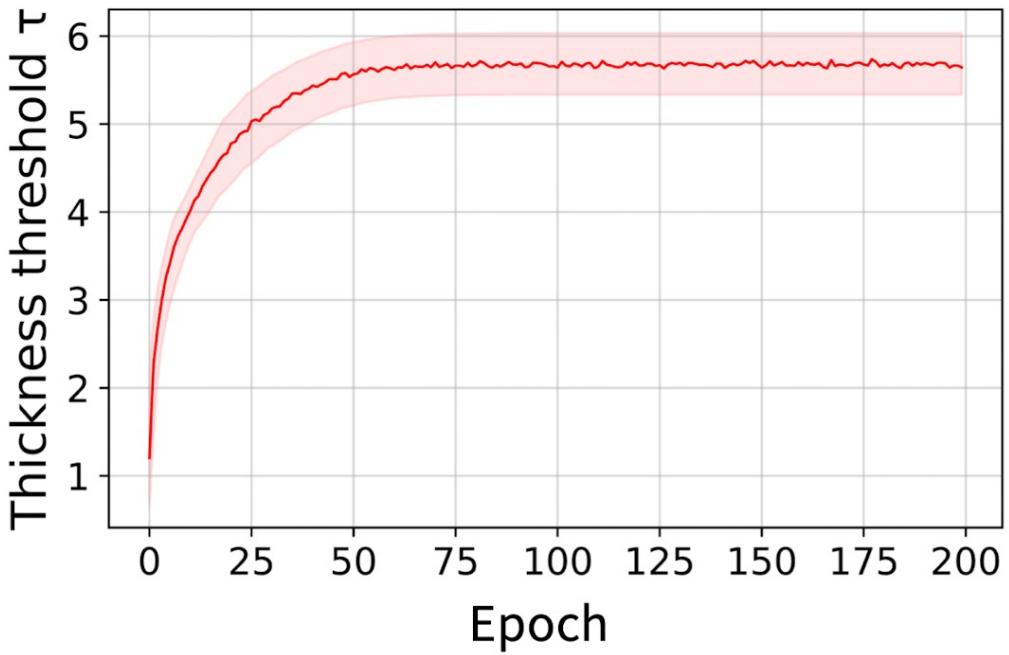

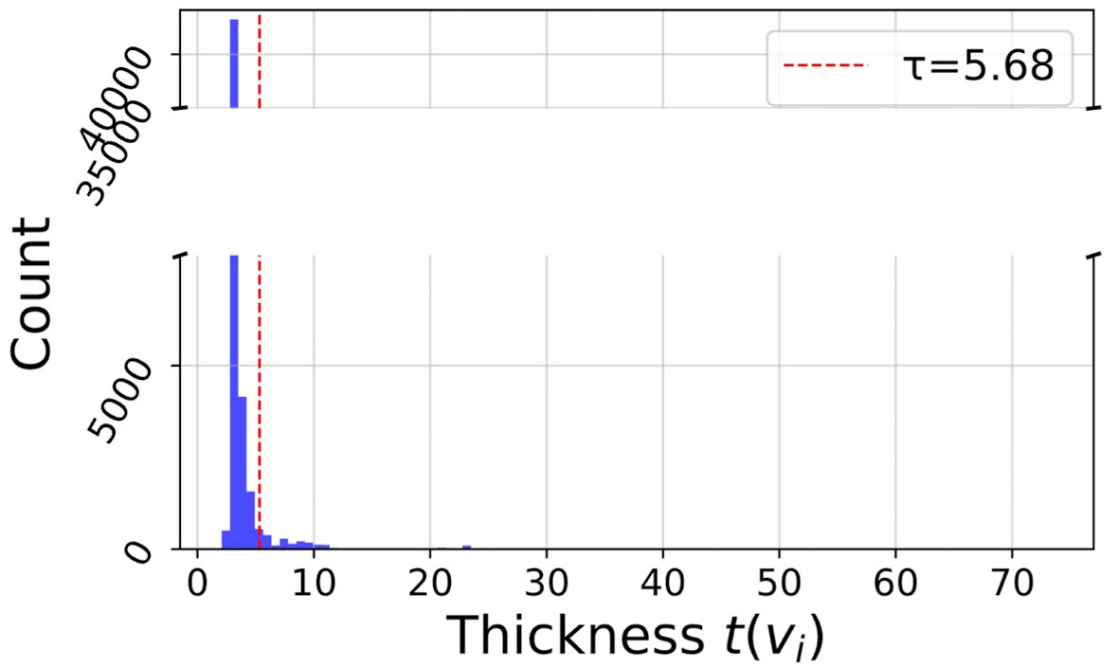

PROPOSED METHOD

- **Core Idea 1: Thickness-Awareness**

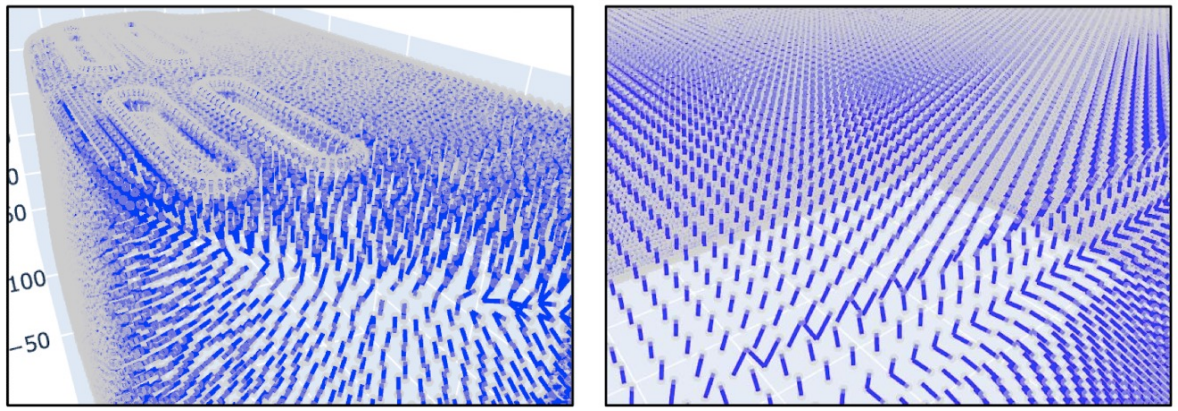

(a) Below the threshold τ

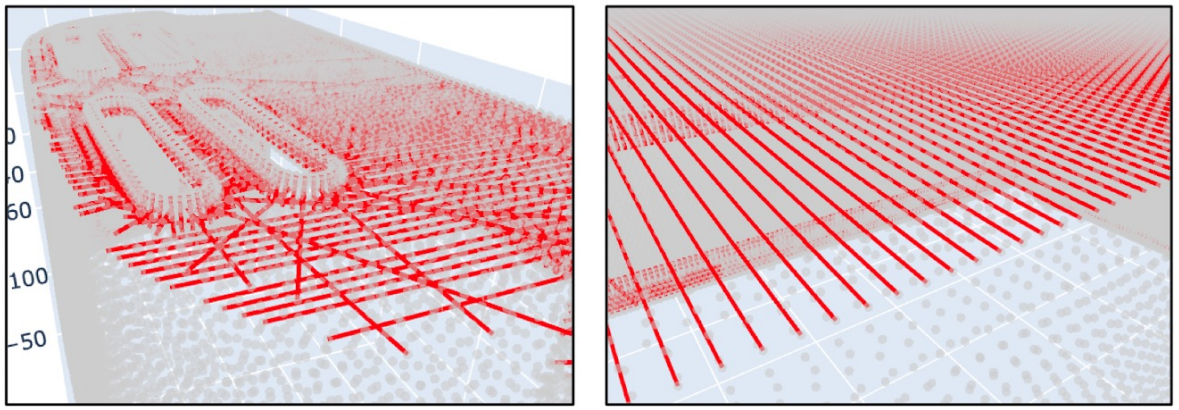

(b) Above the threshold τ

PROPOSED METHOD

- **Core Idea 2: E(3)-Equivariance**

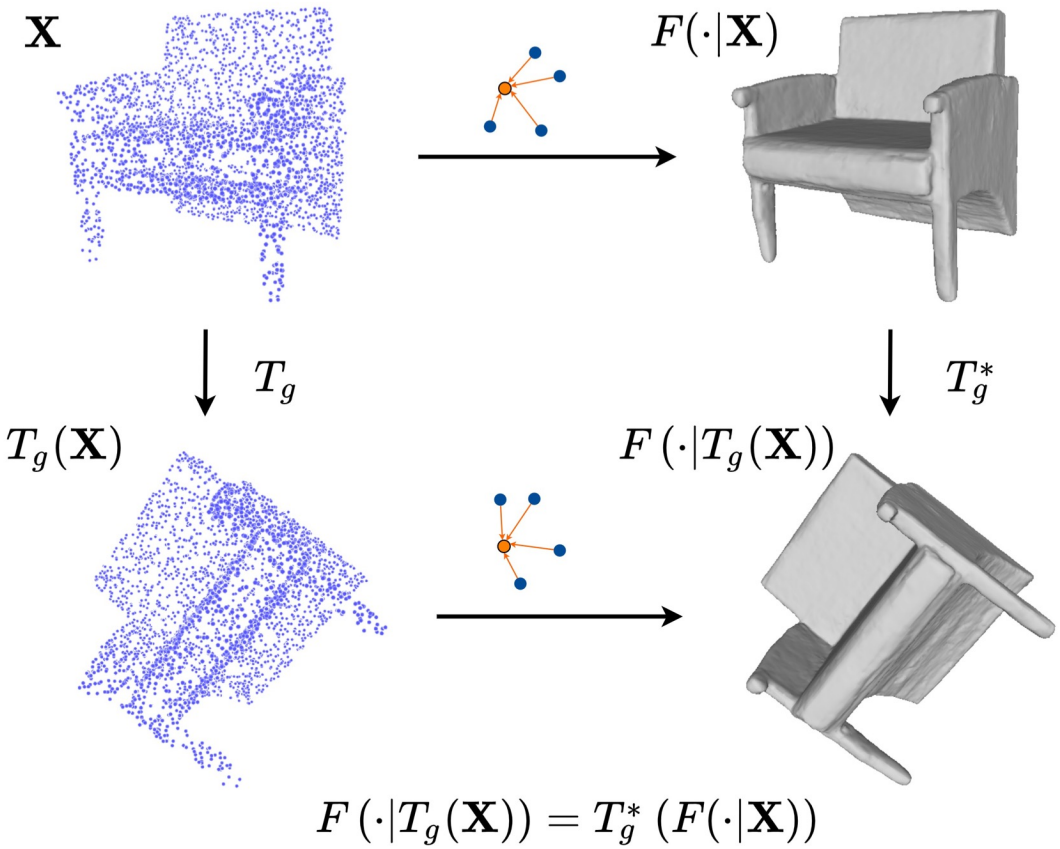

Equivariant Implicit Functions

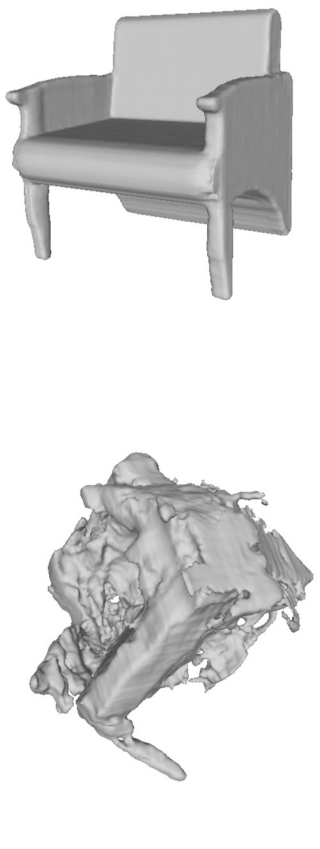

w/o equivariance

Chen, Yunlu, et al. "3d equivariant graph implicit functions." *European Conference on Computer Vision*. Cham: Springer Nature Switzerland, 2022.

PROPOSED METHOD

- **Core Idea 2: E(3)-Equivariance**

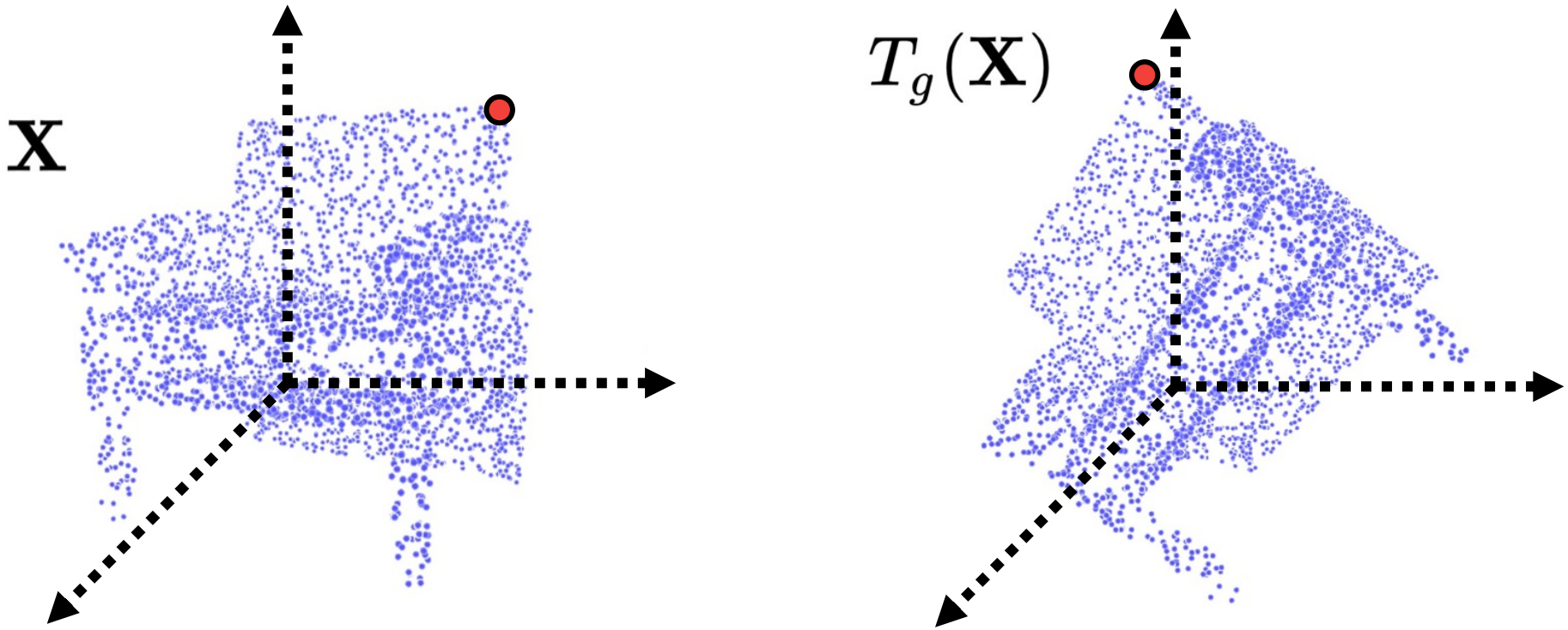

$\phi(\bullet) \neq \phi(T_g(\bullet))$ ϕ: Coordinate encoder

Chen, Yunlu, et al. "3d equivariant graph implicit functions." *European Conference on Computer Vision*. Cham: Springer Nature Switzerland, 2022.

PROPOSED METHOD

- **Core Idea 2: E(3)-Equivariance**

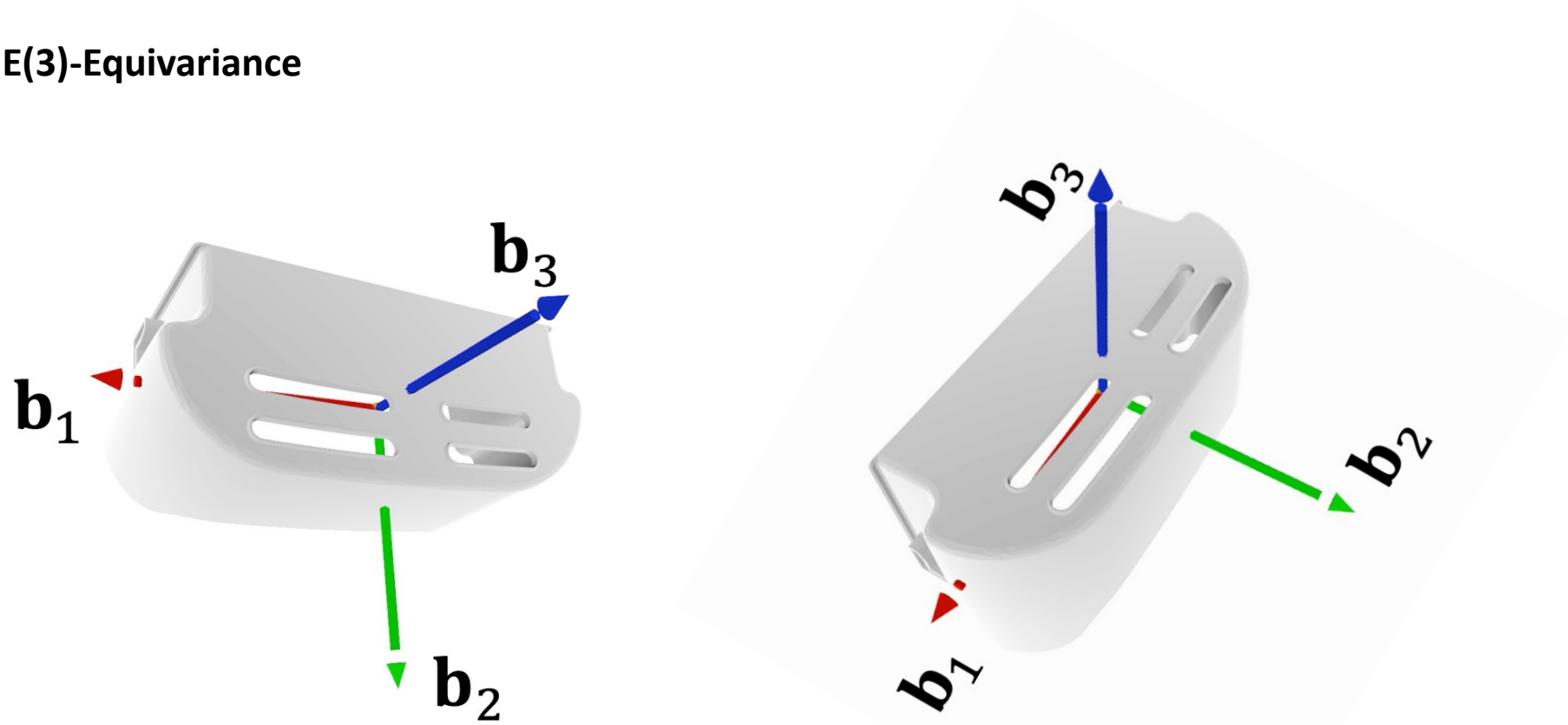

Our proposed **data-driven coordinate system is invariant to E(3) transformations**, which include rotations, translations, and reflections.

PROPOSED METHOD

- **Core Idea 2: E(3)-Equivariance**

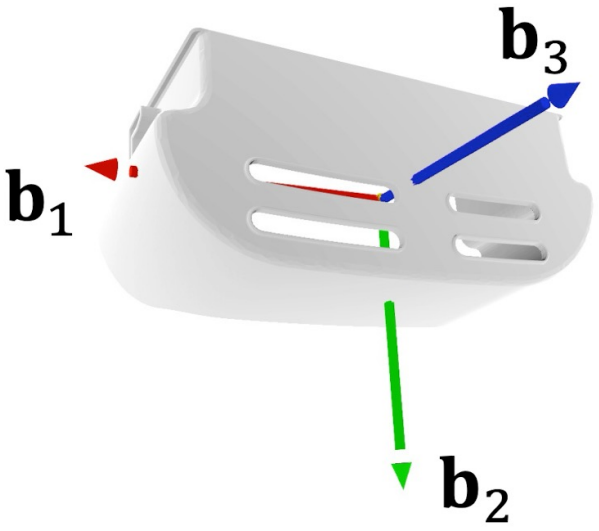

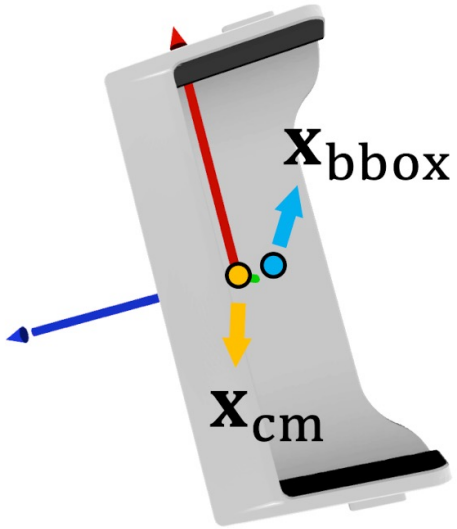

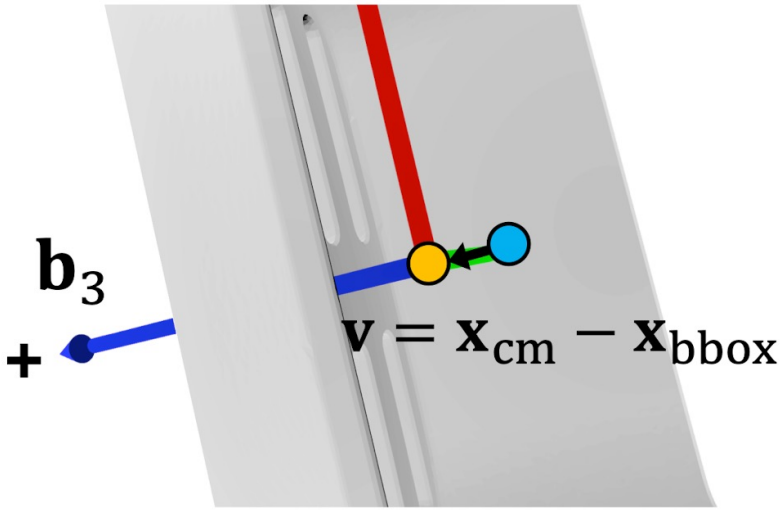

Our proposed **data-driven coordinate system is invariant to E(3) transformations**, which include rotations, translations, and reflections.

PROPOSED METHOD

- **Overall Architecture**

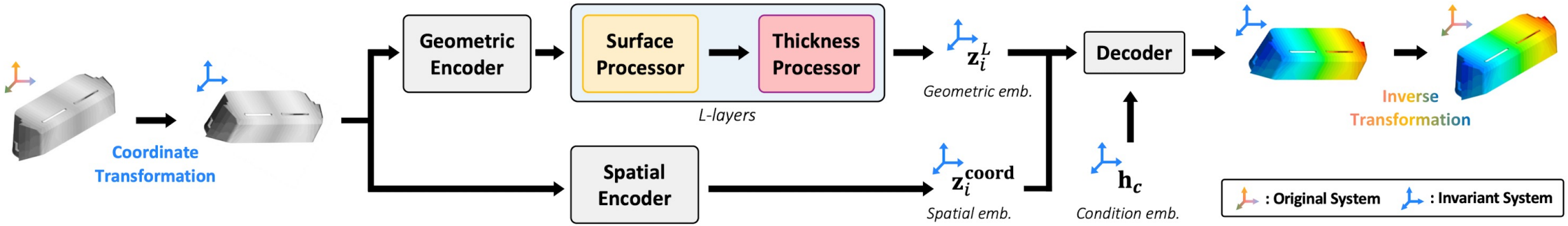

PROPOSED METHOD

▸ **Overall Architecture**

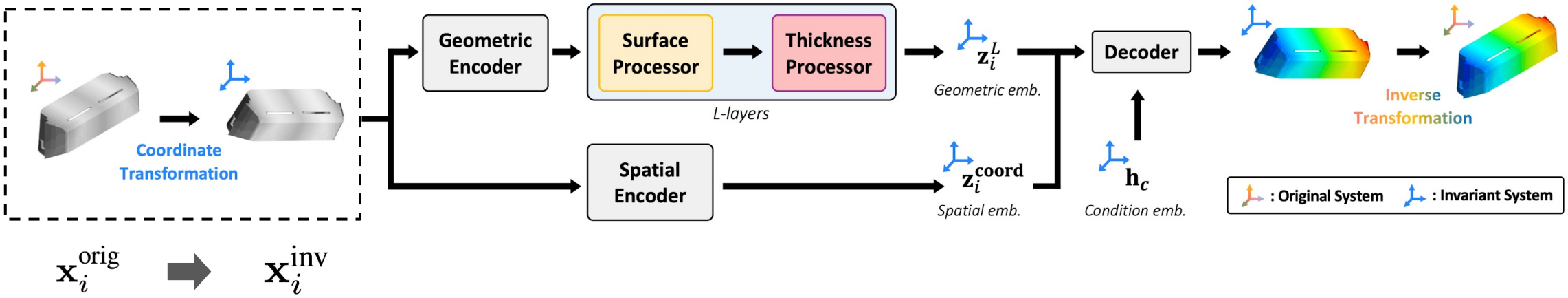

Step 1. Translate the original coordinates relative to the center of mass $\mathbf{x}_{\text{cm}}$ $\quad \tilde{\mathbf{x}}_i = \mathbf{x}_i^{\text{orig}} - \mathbf{x}_{\text{cm}}$

Step 2. The adjusted coordinates are **rotated** to align with the data-driven principal axes. $\quad \mathbf{x}_i^{\text{inv}} = \mathbf{R}^\top \tilde{\mathbf{x}}_i$

* For each shape, the center of mass ($\mathbf{x}_{\text{cm}}$) and the rotation matrix ($\mathbf{R}$) are stored for the inverse transformation.

PROPOSED METHOD

▸ **Overall Architecture**

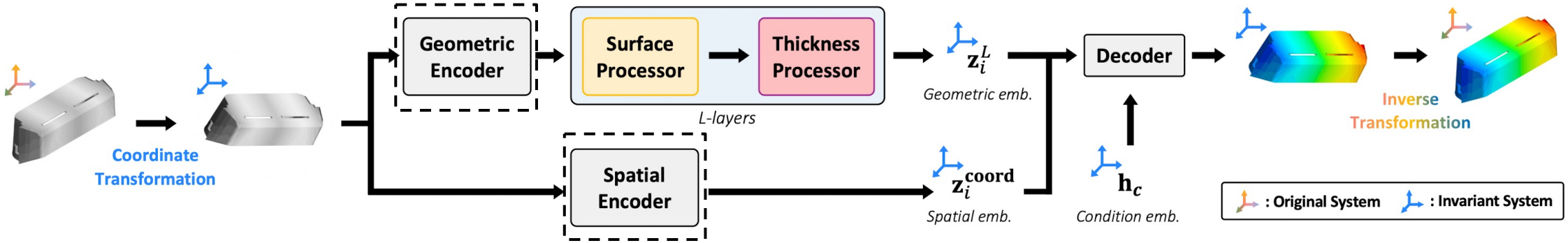

- Geometric Encoder: $\mathbf{z}_i^{(0)} = \phi_{\text{node}}(\mathbf{f}_i), \quad \mathbf{e}_{ij}^{(0)} = \phi_{\text{edge}}(\mathbf{f}_{ij})$
- Spatial Encoder: $\mathbf{z}_i^{\text{coord}} = \phi_{\text{coord}}(\mathbf{x}_i^{\text{inv}})$

PROPOSED METHOD

▸ **Overall Architecture**

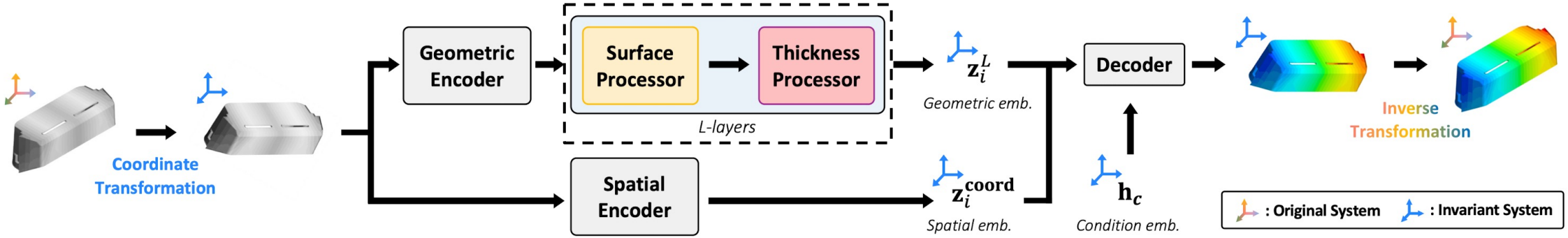

- Surface Encoder:

$$\mathbf{e}_{ij}^{(l+1)} \leftarrow f_{\text{surf}}^{M}(\mathbf{e}_{ij}^{(l)}, \mathbf{z}_i^{(l)}, \mathbf{z}_j^{(l)}),$$

$$\mathbf{z}_i^{\text{surf},(l)} \leftarrow f_{\text{surf}}^{V}(\mathbf{z}_i^{(l)}, \sum_{j \in \mathcal{N}(i)} \mathbf{e}_{ij}^{(l+1)})$$

- Thickness Processor:

$$I_i = \frac{1}{1 + e^{\alpha(t(v_i) - \tau)}} \qquad \mathbf{e}_{i,\text{thick}}^{(0)} \leftarrow \phi_{\text{thick}}(\mathbf{f}_{i,\text{thick}}) \qquad \mathbf{f}_{i,\text{thick}} = [t(v_i), \mathbf{n}_i \cdot \mathbf{n}_{i_{\mathcal{T}}}]$$

$$\mathbf{e}_{i,\text{thick}}^{(l+1)} \leftarrow I_i \cdot f_{\text{thick}}^{M}(\mathbf{e}_{i,\text{thick}}^{(l)}, \mathbf{z}_i^{\text{surf},(l)}, \mathbf{z}_{\mathcal{T}(v_i)}^{\text{surf},(l)})$$

$$\mathbf{z}_i^{(l+1)} \leftarrow f_{\text{thick}}^{V}(\mathbf{z}_i^{\text{surf},(l)}, \mathbf{e}_{i,\text{thick}}^{(l+1)})$$

PROPOSED METHOD

▸ **Overall Architecture**

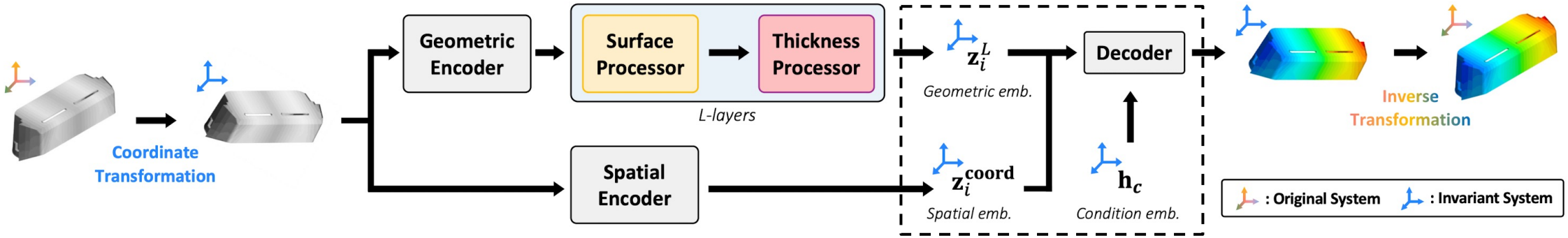

- Decoder: $\mathbf{z}_i^{\text{final}} = \phi_{\text{combine}}([\mathbf{z}_i, \mathbf{z}_i^{\text{coord}}])$

$\mathbf{p}_i^{\text{inv}} = \phi_{\text{decode}}([\mathbf{z}_i^{\text{final}}, \mathbf{h}_c])$

PROPOSED METHOD

▸ **Overall Architecture**

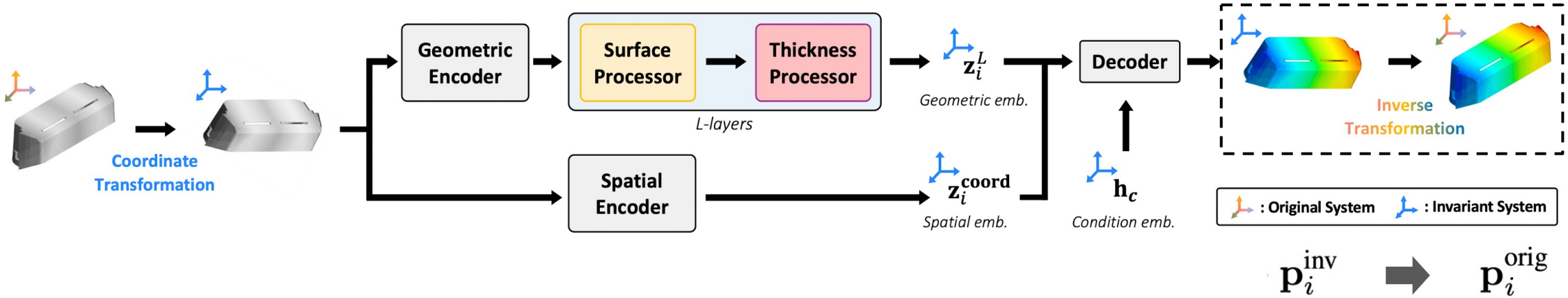

- Inverse Transform: $\mathbf{p}_i^{\text{orig}} = \mathbf{R} \cdot \mathbf{p}_i^{\text{inv}} + \mathbf{x}_{\text{cm}}$

EXPERIMENTAL SETUP

- **Dataset: Real-world injection molding dataset (basket)**

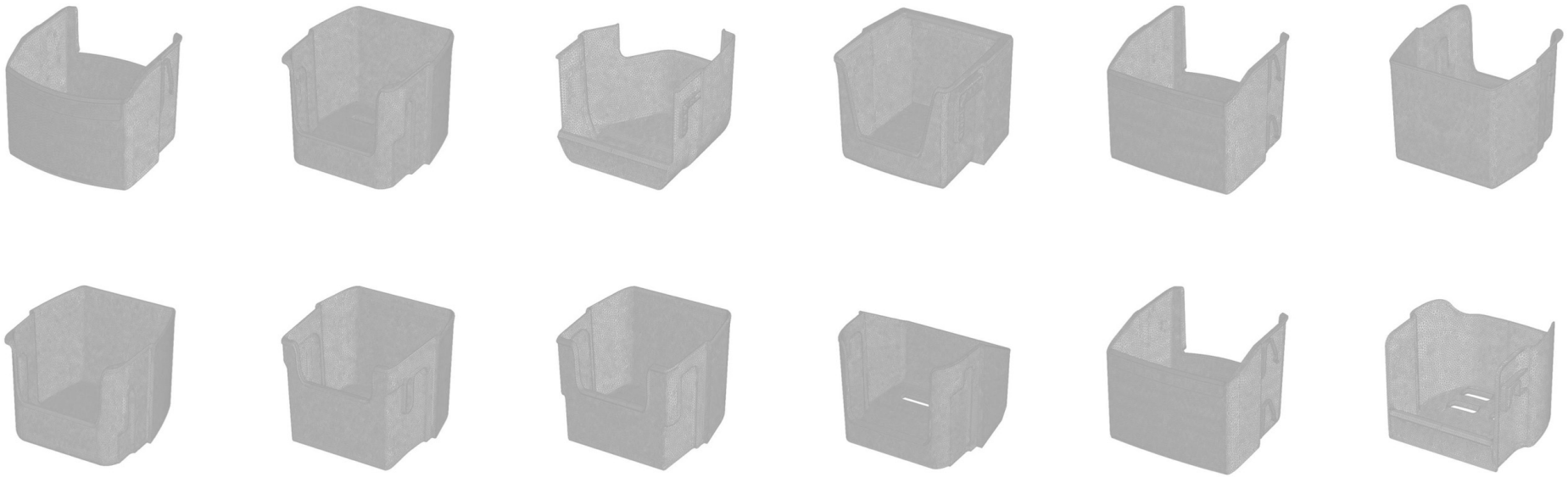

- 28 unique geometries, each with 18 experimental conditions
  - **Test set**
    - Unseen geometries + Seen 18 experimental conditions
    - Seen geometries + Unseen experimental conditions
  - **Out-of-distribution test set**: randomly rotated geometries
- Target: Node-level deflection (3-dimensions prediction for each node)

EXPERIMENTS

- **Result 1: Quantitative Analysis**

Model	Equivariance	Spatial information	Thickness edges	Input of ϕ_{coord}	Edge Feature $\mathbf{f}_{\text{ij}}$	Node Feature $\mathbf{f}_{\text{i}}$	In Distribution (Original)			Out of Distribution (Rotated)		
							RMSE (↓)	MAE (↓)	R^2 (↑)	RMSE (↓)	MAE (↓)	R^2 (↑)
(a) MLP	×	✓	×	-	-	$\mathbf{x}^{\text{orig}}$	0.2818 (0.0061)	0.1164 (0.0035)	0.8984 (0.0029)	0.4789 (0.0181)	0.1939 (0.0070)	0.7393 (0.0248)
(b) MLP	✓	✓	×	-	-	$\mathbf{x}^{\text{inv}}$	0.2546 (0.0015)	0.1043 (0.0008)	0.9154 (0.0016)	0.2545 (0.0015)	0.1071 (0.0007)	0.9385 (0.0009)
(c) MGN	×	×	×	-	$\mathbf{x}_{ij}, \|\mathbf{x}_{ij}\|$	$\mathbf{n}_i, g_i, r_i$	1.2608 (0.0107)	0.5607 (0.0041)	0.0782 (0.0315)	1.3188 (0.0164)	0.6199 (0.0064)	-0.0903 (0.0315)
(d) MGN	×	✓	×	$\mathbf{x}^{\text{orig}}$	$\mathbf{x}_{ij}, \|\mathbf{x}_{ij}\|$	$\mathbf{n}_i, g_i, r_i$	0.2854 (0.0046)	0.1176 (0.0017)	0.8724 (0.0037)	0.4514 (0.0190)	0.1938 (0.0067)	0.7917 (0.0180)
(e) MGN	✓	✓	×	$\mathbf{x}^{\text{inv}}$	$\mathbf{x}_{ij}, \|\mathbf{x}_{ij}\|$	$\mathbf{n}_i, g_i, r_i$	0.2241 (0.0042)	0.0938 (0.0029)	0.9113 (0.0099)	0.2241 (0.0042)	0.0965 (0.0024)	0.9446 (0.0033)
(f) EGNN	✓	×	×	-	$\|\mathbf{x}_{ij}\|$	g_i, r_i	153.051 (4.2992)	54.363 (2.1000)	-14341.0 (1214.1)	196.343 (1.6422)	89.049 (1.2804)	-32260.9 (1039.3)
(g) EGNN	×	✓	×	$\mathbf{x}^{\text{orig}}$	$\|\mathbf{x}_{ij}\|$	g_i, r_i	0.2944 (0.0045)	0.1220 (0.0021)	0.8680 (0.0056)	0.4576 (0.0184)	0.1958 (0.0064)	0.8074 (0.0206)
(h) EGNN	✓	✓	×	$\mathbf{x}^{\text{inv}}$	$\|\mathbf{x}_{ij}\|$	g_i, r_i	0.2270 (0.0019)	0.0963 (0.0008)	0.9129 (0.0026)	0.2271 (0.0019)	0.0987 (0.0009)	0.9443 (0.0012)
(i) EMNN	✓	×	×	-	$\|\mathbf{x}_{ij}\|$	g_i, r_i	166.077 (1.5226)	58.467 (2.0000)	-16034.0 (975.8)	201.450 (1.7433)	92.237 (1.3366)	-34302.7 (644.62)
(j) EMNN	×	✓	×	$\mathbf{x}^{\text{orig}}$	$\|\mathbf{x}_{ij}\|$	g_i, r_i	0.3056 (0.0246)	0.1284 (0.0131)	0.8626 (0.0052)	0.4668 (0.0180)	0.2024 (0.0092)	0.7972 (0.0097)
(k) EMNN	✓	✓	×	$\mathbf{x}^{\text{inv}}$	$\|\mathbf{x}_{ij}\|$	g_i, r_i	0.2210 (0.0057)	0.0937 (0.0034)	0.9149 (0.0034)	0.2210 (0.0057)	0.0963 (0.0052)	0.9473 (0.0012)
(l) T-EMNN	✓	✓	✓	$\mathbf{x}^{\text{inv}}$	$\|\mathbf{x}_{ij}\|$	g_i, r_i	**0.2132** (0.0046)	**0.0892** (0.0025)	**0.9228** (0.0063)	**0.2131** (0.0046)	**0.0918** (0.0023)	**0.9513** (0.0031)

T-EMNN outperformed the other baselines thanks to two key components: **our thickness address** and our **data-driven coordinate** system, which conferred equivariance on both our method and the baselines in OOD settings.

EXPERIMENTS

- **Result 2: Thickness Framework Validation**

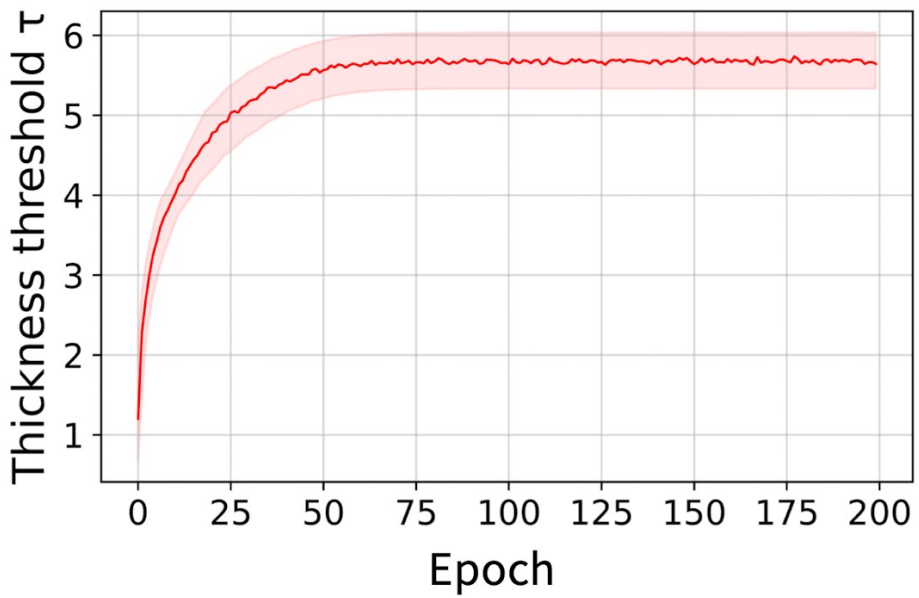

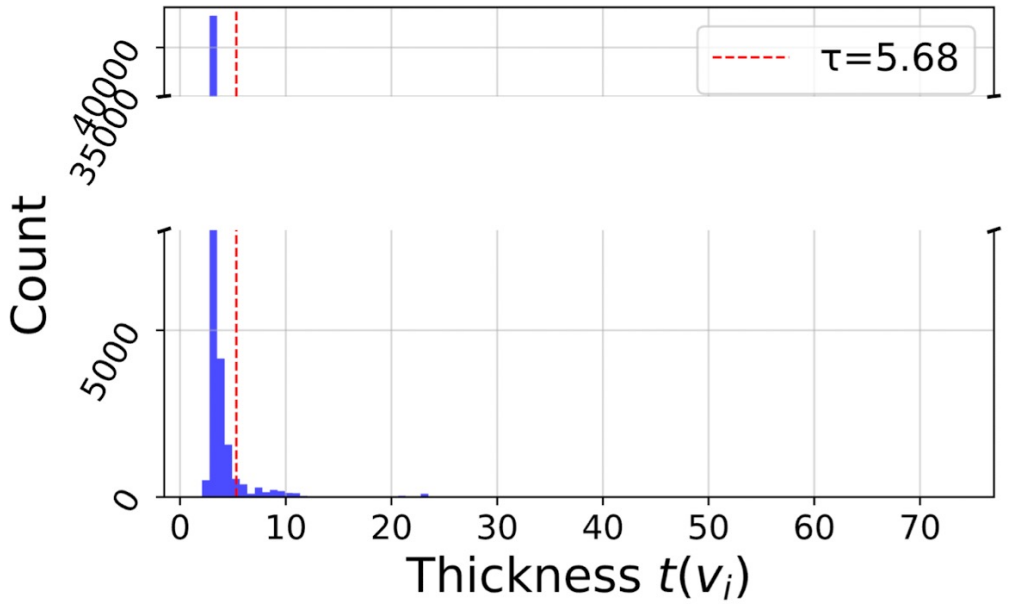

The learnable thickness threshold **converges to a specific value**, which enables interaction between highly correlated nodes on opposing surfaces.

EXPERIMENTS

- **Result 2: Thickness Framework Validation**

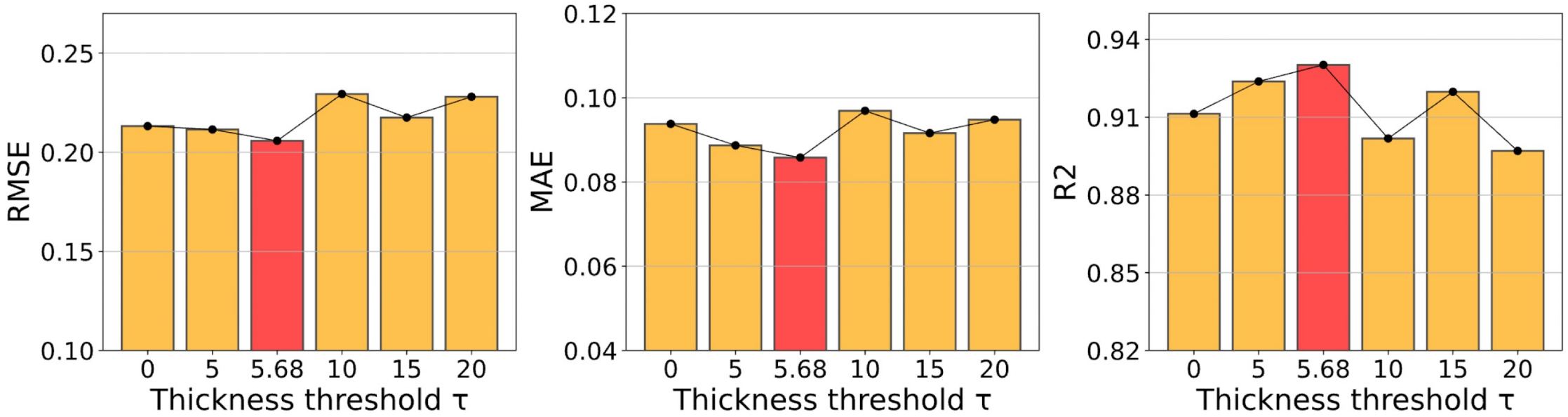

The learned thickness threshold (i.e., 5.68) outperforms the use of manually set, fixed threshold values (e.g., 0, 5, 10, 15, 20).

EXPERIMENTS

- **Result 2: Thickness Framework Validation**

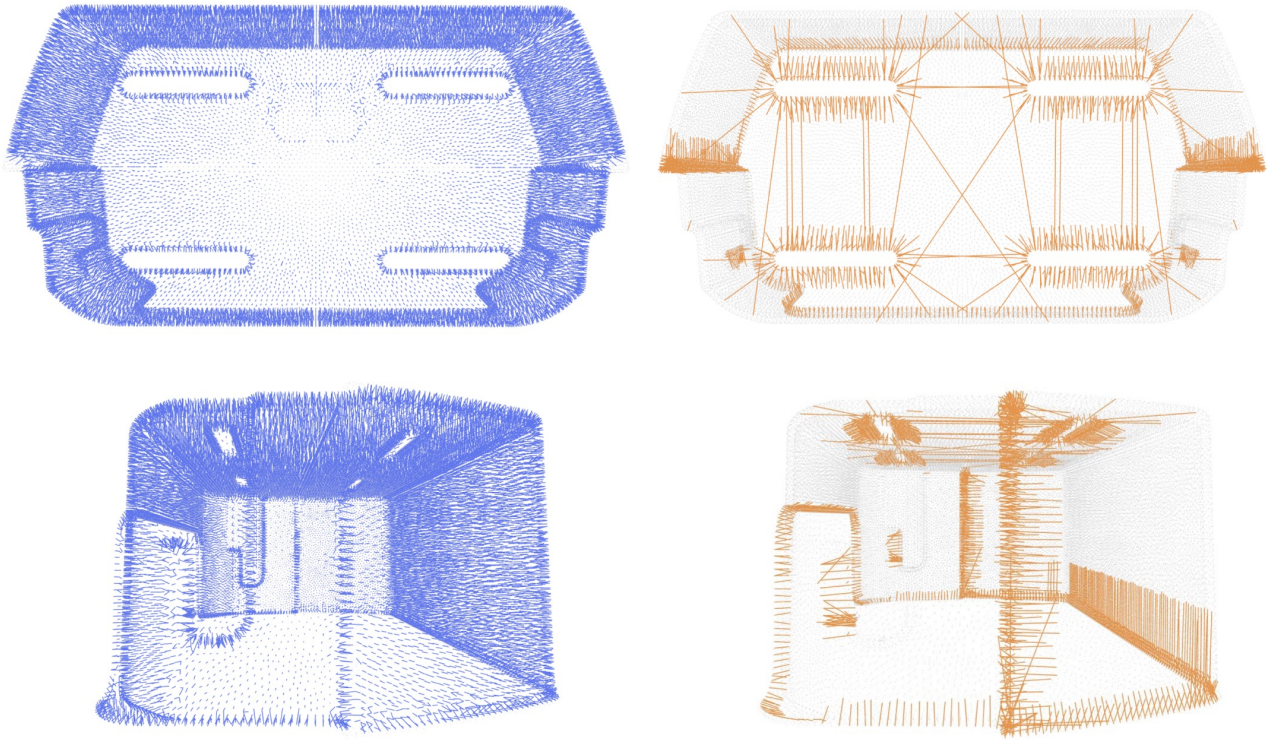

Below the threshold τ Above the threshold τ

The learned thickness threshold (i.e., 5.68) effectively **filters out noisy thickness edges** that can be seen as width rather than thickness.

EXPERIMENTS

- **Result 2: Thickness Framework Validation**

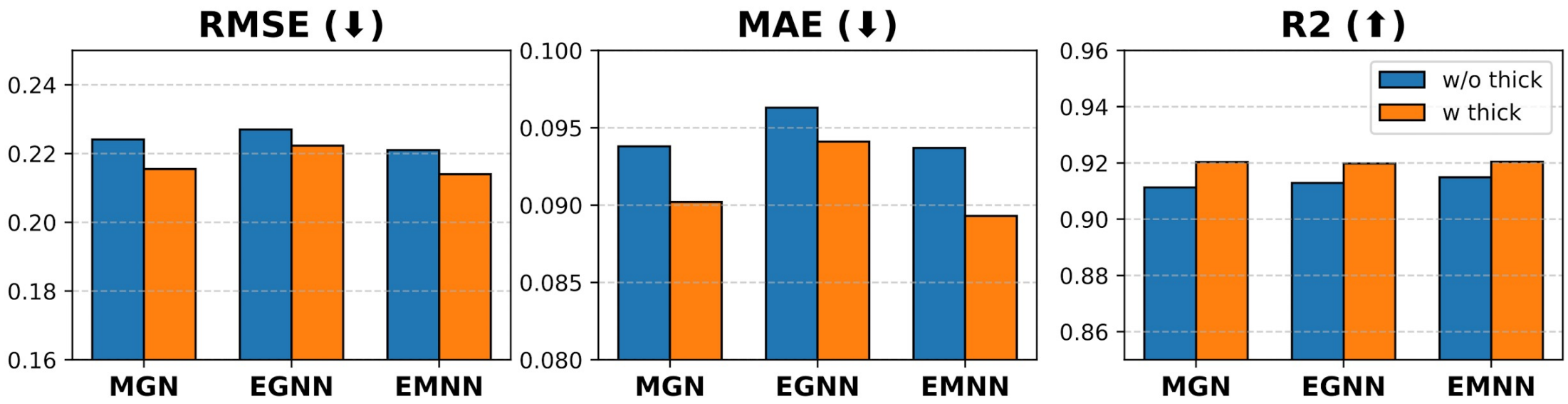

Applying the filtered thickness edges to the baselines improves their performance.

EXPERIMENTS

- **Result 3: Qualitative Analysis**

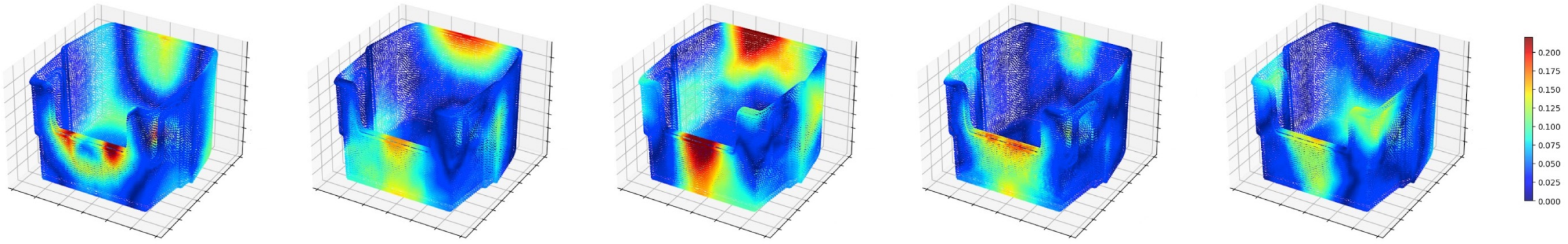

(b) MLP + $\mathbf{x}^{\text{inv}}$ (c) MGN + $\mathbf{x}^{\text{inv}}$ (d) EGNN + $\mathbf{x}^{\text{inv}}$ (e) EMNN + $\mathbf{x}^{\text{inv}}$ (f) T-EMNN

Using thickness edges **reduces the overall error** by allowing messages to pass more effectively between opposing surfaces.

EXPERIMENTS

- **Result 3: Qualitative Analysis**

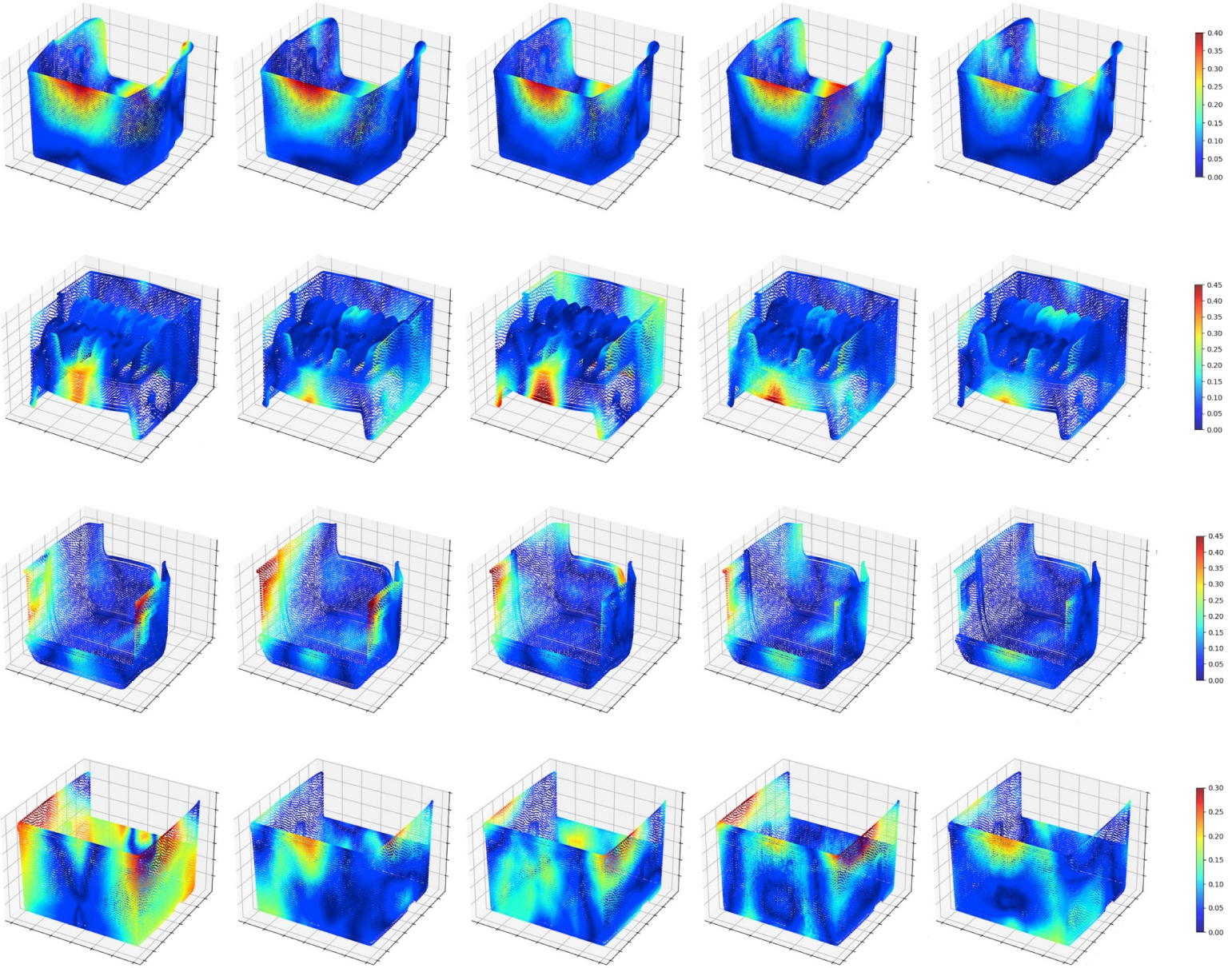

CONCLUSIONS

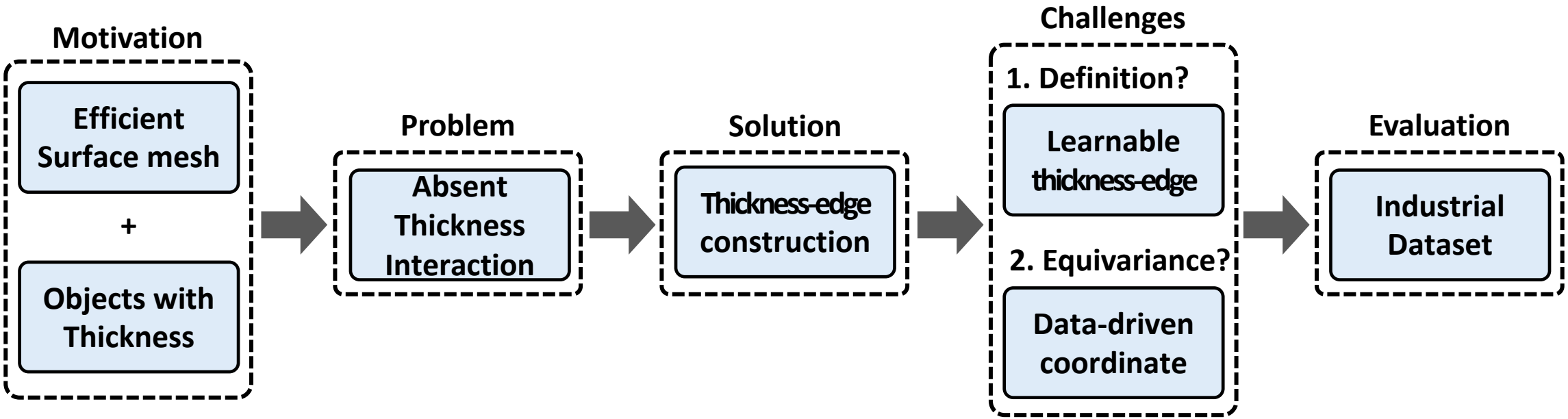

Paper

Thickness-aware E(3)-Equivariant 3D Mesh Neural Network

Paper: https://arxiv.org/abs/2505.21572

Email: swkim@kaist.ac.kr